

## **The Physical Basis for the Lg/P Discriminant: General Properties and Preliminary Modeling**

**Theron J. Bennett  
Keith L. McLaughlin  
Margaret E. Marshall  
Jeffrey L. Stevens**

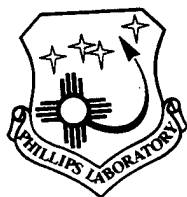
**Maxwell Technologies, Inc.  
8888 Balboa Ave.  
San Diego, CA 92123-1506**

**March, 1997**

**Scientific Report No. 1**

19980519 034

**Approved for public release; distribution unlimited**



**PHILLIPS LABORATORY  
Directorate of Geophysics  
AIR FORCE MATERIEL COMMAND  
HANSCOM AIR FORCE BASE, MA 01731-3010**

**DTIC QUALITY INSPECTED 2**

SPONSORED BY  
Air Force Technical Applications Center  
Directorate of Nuclear Treaty Monitoring  
Project Authorization T/5101

MONITORED BY  
Phillips Laboratory  
CONTRACT No. F19628-95-C-0107

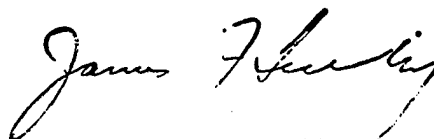
The views and conclusions contained in this document are those of the authors and should not be interpreted as representing the official policies, either express or implied, of the Air Force or U.S. Government.

This technical report has been reviewed and is approved for publication.



---

DELAINE R. REITER  
Contract Manager  
Earth Sciences Division



---

JAMES F. LEWKOWICZ  
Director  
Earth Sciences Division

This report has been reviewed by the ESD Public Affairs Office (PA) and is releasable to the National Technical Information Service (NTIS).

Qualified requestors may obtain copies from the Defense Technical Information Center. All others should apply to the National Technical Information Service.

If your address has changed, or you wish to be removed from the mailing list, or if the addressee is no longer employed by your organization, please notify PL/IM, 29 Randolph Road, Hanscom AFB, MA 01731-3010. This will assist us in maintaining a current mailing list.

Do not return copies of this report unless contractual obligations or notices on a specific document requires that it be returned.

REPORT DOCUMENTATION PAGE			Form Approved OMB No. 0704-0188	
Public reporting burden for this collection of information is estimated to average 1 hour per response, including the time for reviewing instructions, searching existing data sources, gathering and maintaining the data needed, and completing and reviewing the collection of information. Send comments regarding this burden estimate or any other aspect of this collection of information, including suggestions for reducing this burden, to Washington Headquarters Services, Directorate for Information Operations and Reports, 1215 Jefferson Davis Highway, Suite 1204, Arlington, VA 22202-4302, and to the Office of Management and Budget, Paperwork Reduction Project (0704-0188), Washington, DC 20503.				
1. AGENCY USE ONLY (Leave blank)		2. REPORT DATE March, 1997		3. REPORT TYPE AND DATES COVERED Scientific No.1
4. TITLE AND SUBTITLE THE PHYSICAL BASIS FOR THE L <sub>g</sub> /P DISCRIMINANT: GENERAL PROPERTIES AND PRELIMINARY MODELING			5. FUNDING NUMBERS Contract No. F19628-95-C-0107  PE 35999F PR 5101 TA GM WU AG	
6. AUTHOR(S) Theron J. Bennett, Keith L. McLaughlin, Margaret E. Marshall, and Jeffry L. Stevens				
7. PERFORMING ORGANIZATION NAME(S) AND ADDRESS(ES) Maxwell Technologies, Inc. 8888 Balboa Avenue San Diego, CA 92123-1514			8. PERFORMING ORGANIZATION REPORT NUMBER  MFD-FR-97-15727	
9. SPONSORING/MONITORING AGENCY NAME(S) AND ADDRESS(ES) Phillips Laboratory 29 Randolph Road Hanscom AFB, MA 01731-3010  Contract Manager: James C. Battis/VSBI			10. SPONSORING/MONITORING AGENCY REPORT NUMBER  PL-TR-97-2044	
11. SUPPLEMENTARY NOTES				
12a. DISTRIBUTION/AVAILABILITY STATEMENT  Approved for public release; distribution unlimited			12b. DISTRIBUTION CODE	
13. ABSTRACT (Maximum 200 words) A critical problem for reliable implementation of regional discrimination is incomplete understanding of how regional seismic signals depend on physical characteristics of the source and propagation path to the recording station. This research is directed at improving understanding of effects of these characteristics on an important regional discriminant, the L <sub>g</sub> /P ratio. An empirical element in this research program has aimed at describing behavior of L <sub>g</sub> /P ratios and their dependence on frequency for nuclear explosions, earthquakes, rockbursts, and other sources in various tectonic environments. Observations indicate differences between event types which appear to be enhanced at higher frequencies, but sources of scatter in the observations need further study. The theoretical element of this project seeks to explain the main features of the L <sub>g</sub> /P observations in terms of source mechanisms and propagation models for the regional signals. Initial focus of the theoretical studies has been on effectiveness of mechanisms for generation of L <sub>g</sub> by explosive sources. The studies indicate that, even though R <sub>g</sub> -to-L <sub>g</sub> scattering might explain observed frequency dependence and other features of explosion L <sub>g</sub> /P ratios, it probably provides only a minor contribution to explosion L <sub>g</sub> signals compared to other mechanisms.				
14. SUBJECT TERMS Seismic                      Regional                      Spectra                      Source Discrimination              L <sub>g</sub> /P                      Mechanism                      Propagation				15. NUMBER OF PAGES 56
				16. PRICE CODE
17. SECURITY CLASSIFICATION OF REPORT UNCLASSIFIED		18. SECURITY CLASSIFICATION OF THIS PAGE UNCLASSIFIED		19. SECURITY CLASSIFICATION OF ABSTRACT UNCLASSIFIED
				20. LIMITATION OF ABSTRACT UNLIMITED

# Table of Contents

	<u>Page</u>
1. Introduction.....	1
1.1 Objectives.....	1
1.2 Accomplishments.....	2
1.3 Report Organization.....	4
2. Database for Regional Discrimination.....	5
2.1 Availability of Regional Data for Discrimination Studies.....	5
2.2 Event and Station Locations from Historical Database.....	6
3. Analyses of Empirical Data.....	12
3.1 Background for $L_g/P$ Ratios as Discriminants.....	12
3.2 $L_g/P$ Ratio Behavior in the Western U.S.....	14
3.3 $L_g/P$ Ratio Behavior in Eurasia.....	21
3.4 Comparisons Between Regions.....	28
4. Theoretical Basis for Understanding of $L_g/P$ Ratios.....	34
4.1 Modeling Regional Behavior of $L_g$ and P Signals.....	34
4.2 Upper Bounds on the Scattering of $R_g$ into $L_g$ .....	35
5. Summary and Plans.....	42
5.1 Summary of Main Findings.....	42
5.2 Plans for Future Work.....	43
6. References.....	45

## List of Illustrations

	<u>Page</u>
1 Map of western U.S. showing location of NTS relative to regional stations with good digital data which are currently in the database.....	7
2 Map of Eurasia showing location of principal nuclear test sites relative to regional stations with good digital data which are currently in the database...	8
3 Distribution of observations for selected nuclear explosions in western U.S. and Eurasia providing good regional signals in the current database.....	10
4 Distribution with respect to distance of observations for selected earthquakes in western U.S. and Eurasia providing good regional signals in the current database.....	10
5 Distribution with respect to magnitude of observations for nuclear explosions in the western U.S. and Eurasia in the current database.....	11
6 Distribution with respect to magnitude of observations from regional earthquakes in the western U.S. and Eurasia in the current database.....	11
7 Map showing the locations of NTS nuclear explosions and nearby earthquakes relative to the LLNL stations.....	15
8 $L_g/P$ amplitude ratios as a function of frequency at station KNB for NTS underground nuclear explosion tests.....	17
9 $L_g/P$ amplitude ratios as a function of frequency at station KNB for a sample of earthquakes near NTS.....	18
10 Comparison of average $L_g/P$ amplitude ratios as a function of frequency at station KNB for NTS nuclear tests and nearby earthquakes.....	19
11 Comparison of average $L_g/P$ amplitude ratios as a function of frequency from each of the LLNL network stations with overall average for ten NTS underground nuclear explosion tests.....	20
12 Map showing the locations of Soviet nuclear explosions and nearby earthquakes relative to station WMQ in China.....	22

13	$L_g/P$ amplitude ratios as a function of frequency at station WMQ for Shagan River nuclear explosions and earthquakes at similar epicentral distances.....	23
14	Comparison of average $L_g/P$ amplitude ratios as a function of frequency at station WMQ for five Shagan River nuclear tests and five earthquakes at similar distances.....	25
15	Map showing the locations of selected Soviet PNE explosions relative to station BRV.....	26
16	$L_g/P$ amplitude ratios as a function of frequency at station BRV for five PNE tests at epicentral distances less than 1000 km.....	27
17	Comparison of average $L_g/P$ amplitude ratios as a function of frequency for four PNE's at station BRV and five Shagan River nuclear tests at station WMQ recorded at similar epicentral distances.....	29
18	Comparisons of $L_g/P$ amplitude ratios as a function of frequency for selected samples of underground nuclear explosions from several source regions.....	30
19	Comparisons of $L_g/P$ amplitude ratios as a function of frequency for selected samples of earthquakes from several source regions.....	32
20	Comparisons of $L_g/P$ amplitude ratios as a function of frequency for rockbursts from several mining regions.....	33
21	Energy in each mode in three different earth models.....	39
22	Vertical component synthetic seismogram (0.75-1.25 Hz) at a distance of 500 km from a $10^{14}$ Nt-m point explosion source at a depth of 500 km in the EKZ model. The upper panel shows the complete synthetic seismogram. The lower panel shows the P and $L_g$ waveforms at a higher magnification. There is 50 times more spectral amplitude in the $R_g$ than the P wave; however, if all of the $R_g$ seismic energy is converted to incoherent higher mode energy the expected $L_g$ spectral amplitude would only be 270 percent larger than the direct $L_g$ .....	41

## List of Tables

	<u>Page</u>
1 Scattering ratios for three types of distribution among higher modes: equal amplitude, equipartition of energy, and maximum amplitude in a single mode.....	39
2 $L_g/P$ amplitude spectral ratios at 500 km for three models from an explosion point source at a depth of 500 m. In each case, the $R_g \rightarrow L_g$ generated $L_g$ spectral energy is comparable to the $L_g$ energy directly excited by the explosion source.....	39

# 1. Introduction

## 1.1 Objectives

The Comprehensive Test Ban Treaty (CTBT) will require the detection and identification of seismic events down to low magnitudes. This requirement will make it necessary to rely on regional seismic monitoring to locate and identify small events. Although considerable progress has been made over the past decade in understanding the characteristics of regional seismic signals, effective regional discriminants, which can be applied generally, have yet to be determined. The two fundamental problems which remain for regional discrimination are (1) lack of adequate empirical data from different source types and different regions to provide the necessary calibration of regional discrimination techniques, and (2) incomplete understanding of how regional seismic signals depend on physical characteristics of the source and on the propagation environment along the path to the recording station. The goal of this research project is to improve physical understanding of the effects of source and propagation on a specific regional discriminants - viz. the  $L_g/P$  ratio. Over the years, the  $L_g/P$  ratio has proven to be one of the more promising and enduring measures for distinguishing between explosions and earthquakes. By improving understanding of the physical basis for this discriminant, we hope to acquire the knowledge which will enable more reliable application of the discriminant and the extension of regional discrimination capabilities into uncalibrated regions.

To reach this objective, the research program includes an empirical element aimed at determining the characteristic behavior of  $L_g/P$  ratios and their dependence on frequency and distance for the various source types of interest and for different source regions where these observations are available. These empirical observations are then used to constrain theoretical models representing the source types and regional propagation paths. The models which are derived and refined from this process can be used to improve understanding of the physical basis for discriminating events with  $L_g/P$  ratios.



## 1.2 Accomplishments

For use in the empirical element of this research program, we have collected regional waveform data from a variety of source types including nuclear explosions, earthquakes, rockbursts, and chemical blasts for a range of propagation environments. Most regional waveform data for nuclear tests are available from only a few source regions (viz. the Nevada Test Site (NTS) in the United States, the former Soviet test sites at Shagan River (SR) in East Kazakhstan and at Novaya Zemlya (NZ), and the Chinese test site at Lop Nor). To provide a wider range of source and propagation environments, we have sought to supplement the nuclear explosion database with data from additional underground nuclear explosions which were conducted in many areas of the former Soviet Union as part of the Peaceful Nuclear Explosion (PNE) program. For comparison to other source types, we have collected regional data from seismic sources other than nuclear explosions in the same or nearby regions. These data include mainly earthquakes near NTS and elsewhere in the western U.S., earthquakes along the southern border of the former Soviet Union and farther south into China and other neighboring countries, and earthquakes in Europe, Scandinavia, and several other regions. Records from some non-nuclear explosions in a few different source areas are also in the database. In addition, we have included regional seismic data from rockbursts and other mining-induced events from many different regions, such as South Africa, Central Europe, and the eastern and western U.S. We are continuing to supplement the database with more recent events of all types recorded at the modern IDC and other digital stations for areas of interest.

In analyzing the seismic waveform data from these events, we have used both Fourier spectral analyses and band-pass filter analyses of the signals at regional stations to determine amplitudes in group-velocity windows corresponding to  $L_g$  and regional P. Ratios between regional phases (viz.  $L_g/P$ ) at spectral frequencies or at filter center frequencies have been determined; and the spectral ratios were plotted as a function of frequency. We are still experimenting somewhat to determine the most effective ways to measure these regional phase spectra and spectral ratios. Alternative group velocity

windows, frequency bands, and amplitude averaging techniques are being assessed. We are also investigating effects of source region and attenuation on  $L_g/P$  ratios.

Results from our initial investigations are generally in agreement with past findings which indicate that  $L_g/P$  ratios are lower for nuclear explosions than for other types of sources with the largest differences observed at higher frequencies. The ratios for rockbursts and earthquakes tend to be similar, showing relatively high values (near one) over a fairly broad range of high frequencies; while the ratios for nuclear explosions normally fall well below one at high frequencies. Some of our best-controlled observations are from nearer-regional stations surrounding NTS explosions and nearby earthquakes, while our experience from Eurasian explosions and earthquakes generally involves more-distant regional stations. Our results show differences in the  $L_g/P$  ratio behavior with frequency for the same source types from the different sets of observations. The ratios generally show less rapid decline with increasing frequency for NTS explosions than for East Kazakhstan explosions. We have been attempting to determine whether this effect can be explained by attenuation differences or whether source excitation differences might also be a factor.

With regard to theoretical modeling of the behavior of the  $L_g$  and regional P signals from different types of seismic sources, a long-standing problem has been to adequately explain the S or  $L_g$  signals associated with nuclear explosions. Several possible mechanisms for generation of such signals are under consideration; these mechanisms generally can be grouped into two categories: (1) those related to indirect conversion of energy radiated by the isotropic explosion source into S waves, or (2) non-isotropic components added to the explosion to produce a composite source which generates the S waves. We have been attempting to evaluate the effectiveness of several such mechanisms for  $L_g$  generation within some representative crustal models. The crustal models which we have used in these analyses so far include a Gutenberg earth model, along with models for NTS and for the former Soviet test site in East Kazakhstan. One mechanism for  $L_g$  generation from the explosion source which has been analyzed is  $R_g \rightarrow L_g$  scattering. Our initial model studies suggest that this mechanism can possibly explain some of the observed characteristics of regional signals from buried nuclear

explosion sources, but maybe not others. In particular, the model predicts that  $R_g \rightarrow L_g$  scattering for frequencies near 1 Hz is probably as effective as near-source  $P \rightarrow S$  conversions at horizontal interfaces. However, this mechanism may not be capable of producing the relatively large  $L_g/P$  ratios observed from nuclear explosions at frequencies of 1 Hz and lower; and at higher frequencies this mechanism for  $L_g$  generation is quite ineffective. Additional studies of this and other mechanisms for producing the observed behavior of  $L_g/P$  ratios with frequency for explosion sources are currently being pursued. We will ultimately seek to explain the different effects of the explosion and non-explosion mechanisms on this behavior for representative crustal models.

### **1.3 Report Organization**

This report is divided into five sections including these introductory remarks. Section 2 describes the event database which we have been working with. Section 3 discusses the results from the analyses of the empirical data in several different regions. Section 4 describes the modeling studies which have been performed, focusing on investigations of the physical mechanism and efficiency of generation of  $L_g$  signals by explosion sources. Section 5 summarizes the preliminary results and describes the plan for continuing work to determine the physical basis for the  $L_g/P$  regional discriminant.

## **2. Database for Regional Discrimination**

### **2.1 Availability of Regional Data for Discrimination Studies**

Regional recordings of underground nuclear explosions cover a very limited domain in space and time. Over the years the most active test sites have been at NTS in the western U.S., near Shagan River in East Kazakhstan, and Novaya Zemlya in the Russian arctic. In addition, numerous tests were conducted by the former Soviet Union in the North Caspian basin and elsewhere throughout their former territories as part of the Peaceful Nuclear Explosions (PNE) program. France has also detonated numerous nuclear explosions at a site in the South Pacific and, prior to that, in northern Africa. Additional nuclear explosion tests have been conducted in western China at Lop Nor, and there have been scattered events in other source regions. So, while there have been underground nuclear explosions in a variety of geographic areas around the world, there are large portions of the world where there is little or no experience with nuclear tests. In comparison, earthquakes and other seismic sources also occur in many regions throughout the world; but the areas around many of the nuclear explosion test sites are relatively inactive with respect to these alternate sources. As a result, direct empirical comparisons may not be convincing unless a proper physical understanding can be developed to serve as the basis for analyzing regional signals from different source types and propagation regions.

A second factor affecting availability of data for regional discrimination studies is the history of seismic monitoring. The seismic monitoring environment is continually changing as newer, better-quality single stations and arrays are fielded and calibrated. However, because of testing moratoria and the tapering off of the nuclear testing programs in most countries, there are little or no data available from nuclear explosions at many of the more modern stations. The new data alone are inadequate to calibrate regional discrimination capabilities, particularly at the level which would be required for reliable CTBT monitoring. The historical regional data can be useful in helping to infer the characteristics of regional signals from potential nuclear tests in uncalibrated regions. A physical basis for such inferences is critical to understanding the behavior of

discriminant measures and how they are likely to perform in such regions. After establishing the physical basis for regional discrimination, the regional observations for alternative event types from the modern station network can be reassessed to evaluate CTBT event identification capabilities.

## **2.2 Event and Station Locations from Historical Database**

In a previous report (cf. Bennett et al., 1996), we described the characteristics of the regional seismic database of underground nuclear explosions and earthquakes which we have been working with to improve discrimination capability. We also discussed there what additional data from some of these historical seismic stations might be available and useful for supplementing the current database. In this report we will only summarize the database description from our previous study. Traditionally, the best controlled data sample for analyzing the differences between regional signals from nuclear explosions and earthquakes is the large body of regional recordings from NTS nuclear explosions and nearby earthquakes (cf. Murphy and Bennett, 1982; Bennett and Murphy, 1986; Taylor et al., 1989). In the course of our regional discrimination studies over the years, we have collected digital waveform data from selected NTS nuclear explosions and earthquakes in the surrounding regions. In general, we have tried to select earthquakes and explosions for direct comparison which have similar propagation paths, so that attenuation differences would not be a significant factor. As a result, the majority of earthquakes in the database are events with epicenters within about 100 km of NTS. The majority of these earthquakes tend to be small. To provide comparisons at some of the more distant stations, we have relaxed this constraint somewhat and included larger explosions and earthquakes with somewhat greater source separation but still with roughly comparable epicentral distances, and thus similar propagation. Figure 1 shows the locations of the stations in this database for western U.S. events. Much of the data comes from nearer-regional stations; signal-to-noise levels tend to be poor at the farther stations, especially for  $L_g$ , although regional signals are strong in some frequency bands for larger events even at far-regional stations. The map in Figure 2 shows the locations of stations in Eurasia from which we have collected good regional signals from Eurasian

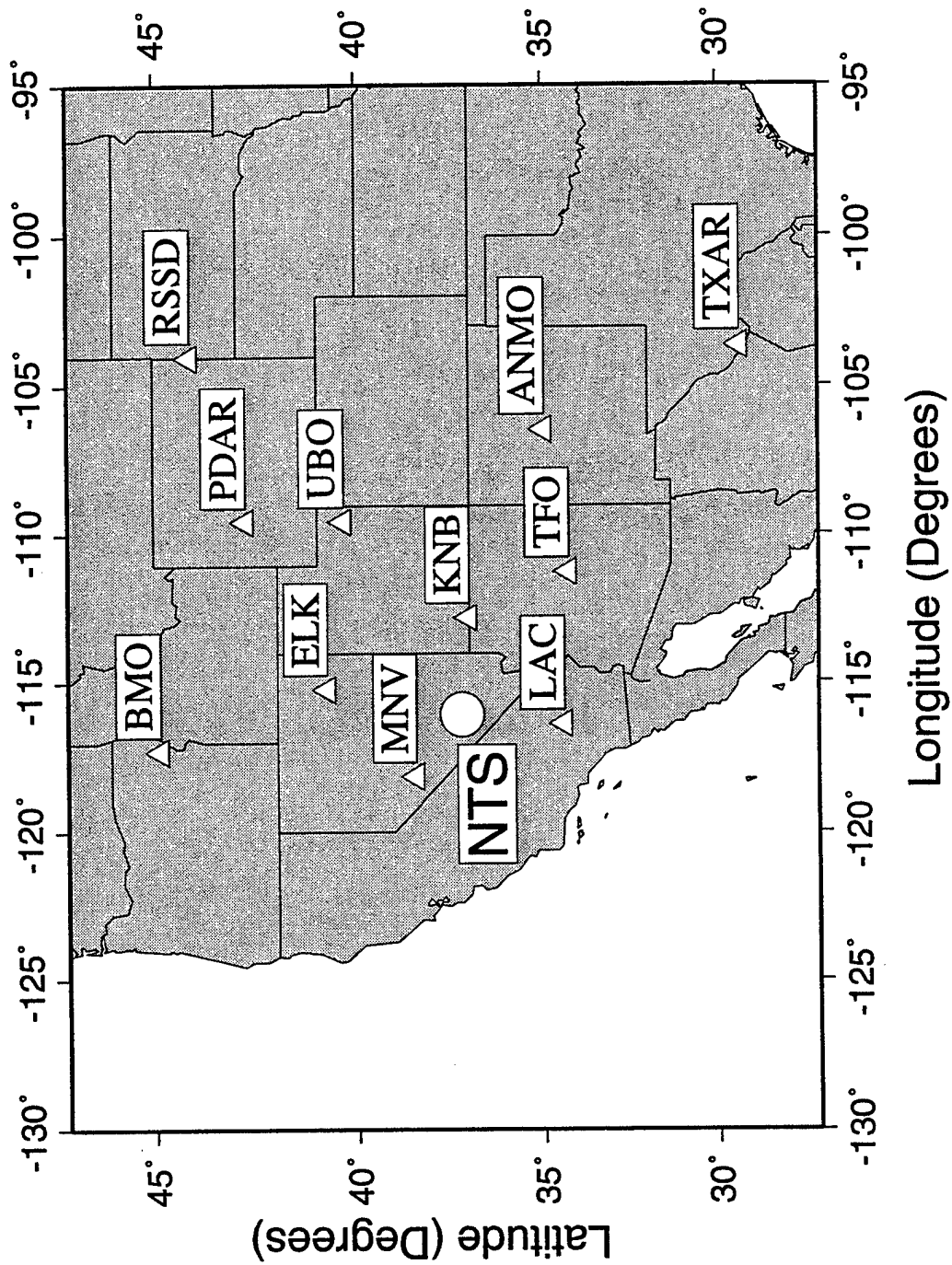


Figure 1. Map of western U.S. showing location of NTS relative to regional stations with good digital data which are currently in the database.

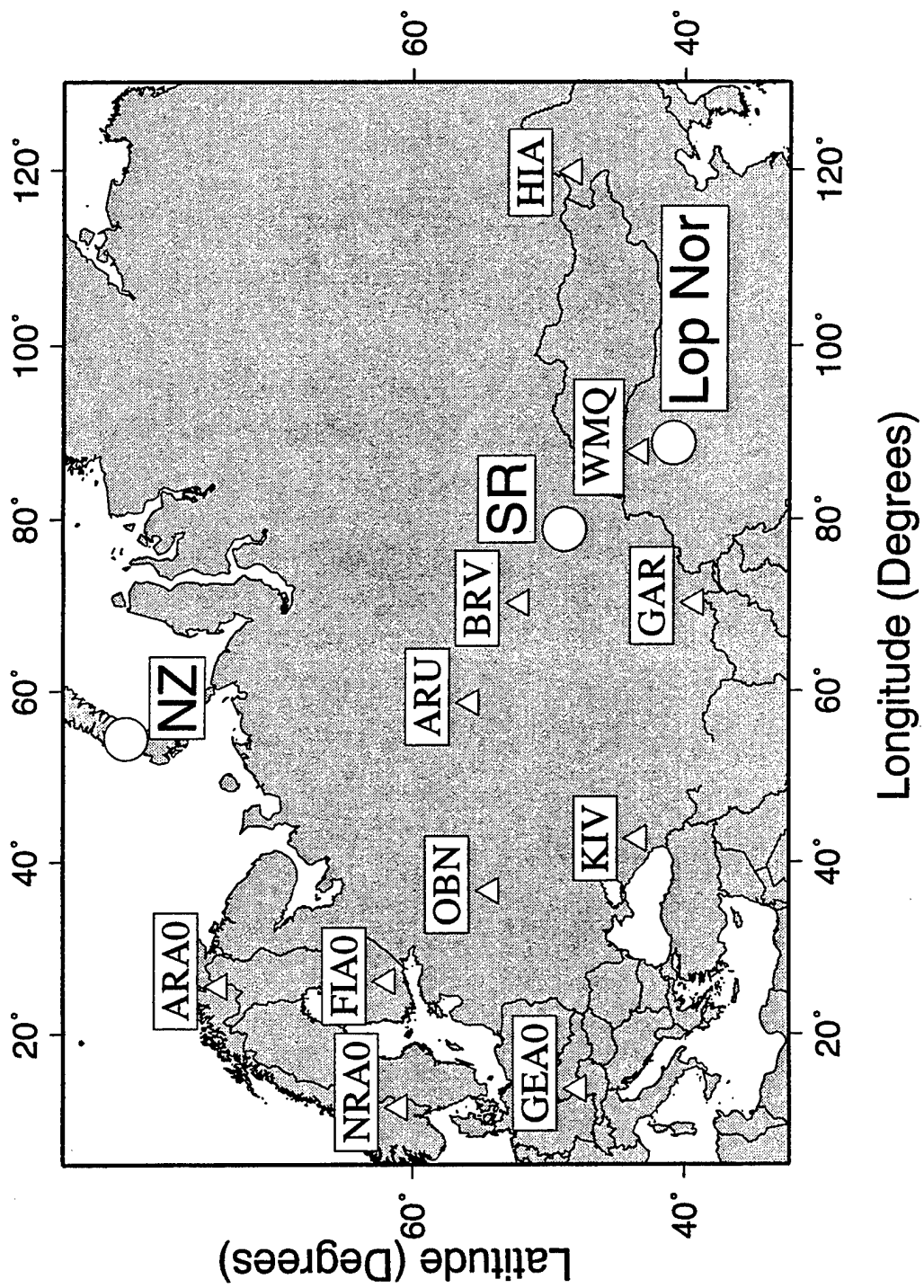


Figure 2. Map of Eurasia showing location of principal nuclear test sites relative to regional stations with good digital data which are currently in the database.

nuclear explosions and earthquakes in the current database. In this case, many of the data come from farther regional stations; the signal-to-noise levels tend to be fairly high on broadband records for many of the larger magnitude events, although the S and  $L_g$  signals sometimes have limited useful bandwidth at these greater distances.

Figures 3 through 6 summarize the distribution of the observations in our regional database with respect to epicentral distance and event magnitude. In this presentation we have combined the samples from the western U.S. and Eurasia; in our prior report (cf. Bennett et al., 1996) we provided separate distributions for these regions and compared between the regions. Figures 3 and 4 show the distributions with respect to epicentral distance for nuclear explosions and earthquakes, respectively. The distributions appear similar with the data concentrated at ranges less than 1000 km for both source types. This is primarily due to the prevalence of nearer-regional stations in the western U.S. database for nuclear explosions. It is noteworthy in this regard that, in assembling the database, we deliberately sought nearby events of similar magnitudes for comparison; and, because most earthquakes occurring near NTS were small, we also sought small explosions which were not necessarily very well recorded at more distant stations. In contrast, the regional data from Eurasian seismic events tend to be concentrated at distance ranges of 1000 km and beyond. This is primarily because the seismic stations available for recording nuclear explosions from the former Soviet Union were generally located at far-regional distances from the principal test sites, and again we sought earthquake observations for comparison which would be at similar epicentral distances.

Figures 5 and 6 show the distributions of the regional data in the database with respect to magnitude for nuclear explosions and earthquakes respectively. The distributions are somewhat similar, although the earthquake distribution tends to be spread over a broader magnitude range and appears to be biased somewhat toward slightly lower magnitudes than the nuclear explosions. This is related to the difficulty alluded to above in trying to find large earthquakes in proximity to the nuclear test sites for use in comparisons. It should be noted, with regard to the  $L_g/P$  ratio discriminant, that such magnitude differences are probably less critical than for the  $L_g$  spectral ratio



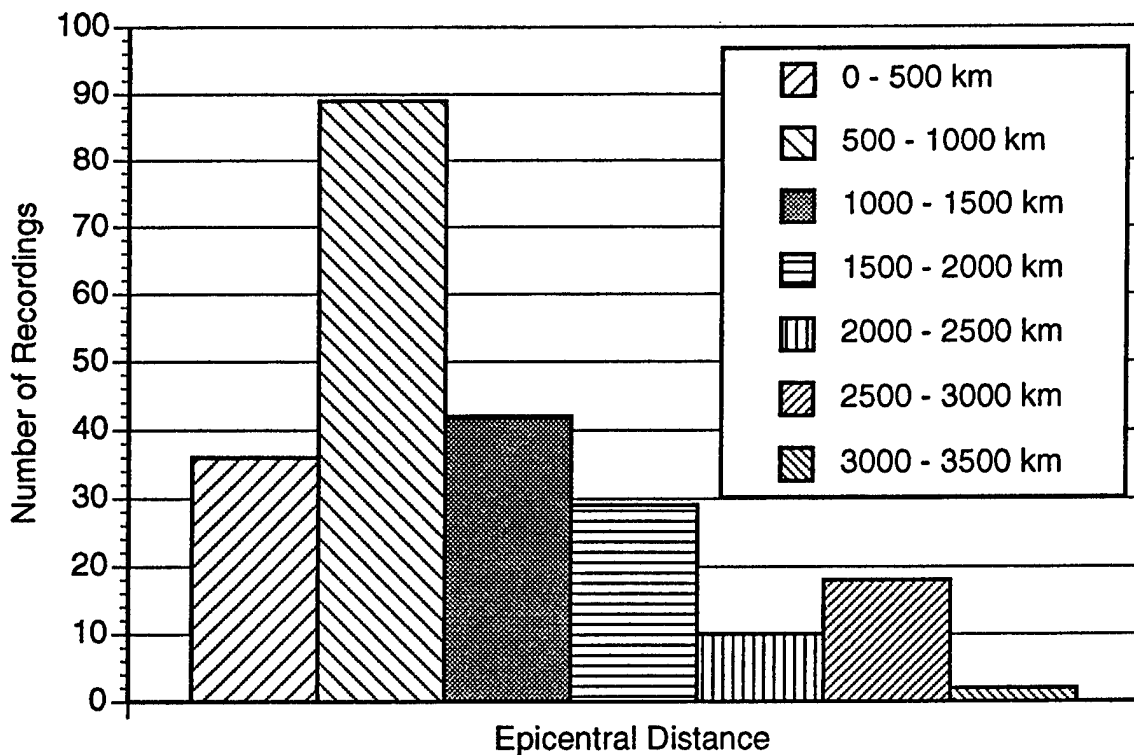


Figure 3. Distribution of observations for selected nuclear explosions in western U.S. and Eurasia providing good regional signals in the current database.

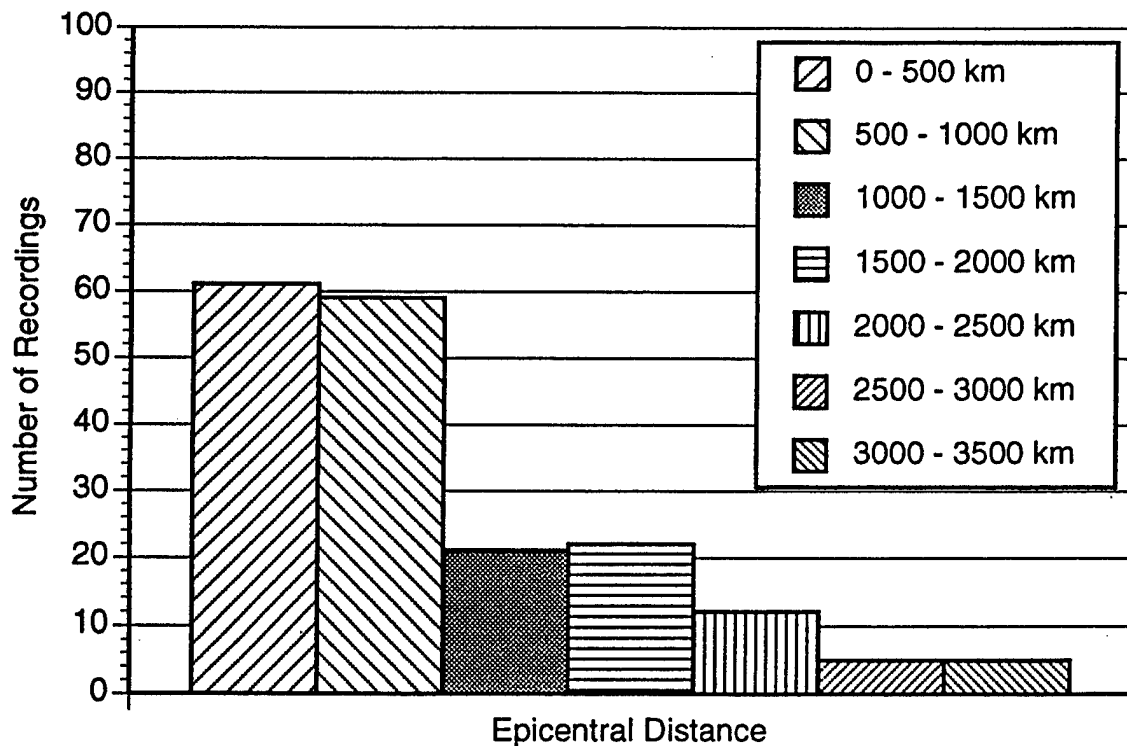


Figure 4. Distribution with respect to distance of observations for selected earthquakes in western U.S. and Eurasia providing good regional signals in the current database.

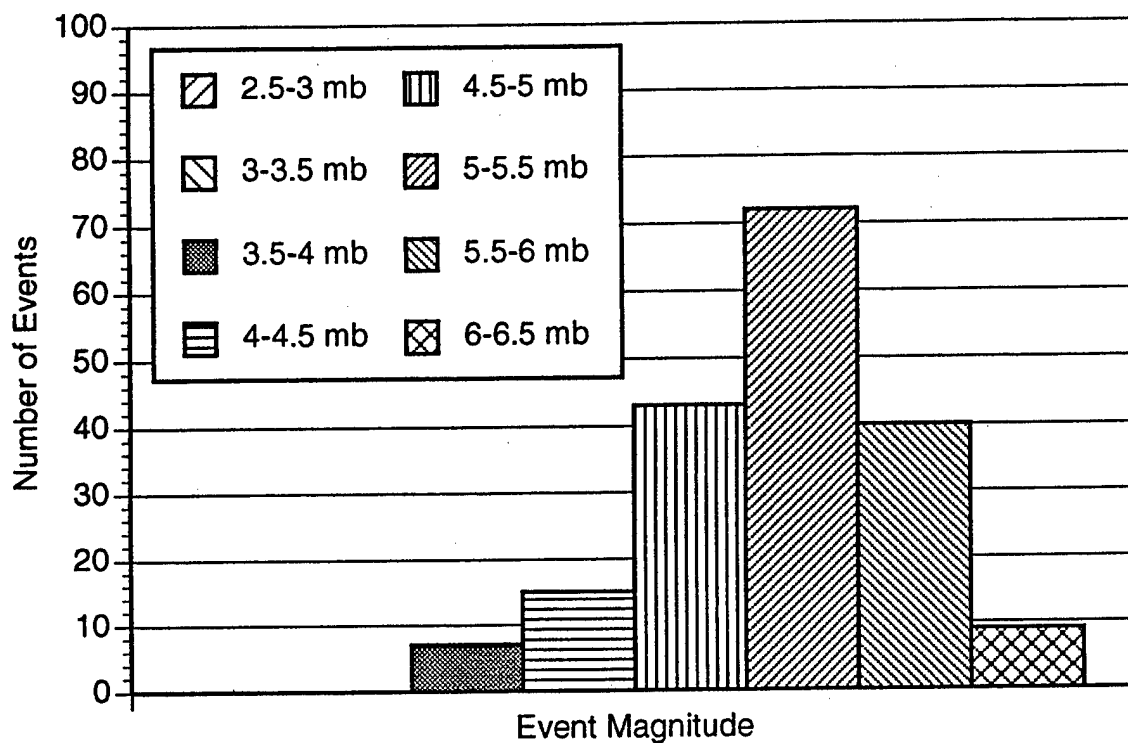


Figure 5. Distribution with respect to magnitude of observations for nuclear explosions in the western U.S. and Eurasia in the current database.

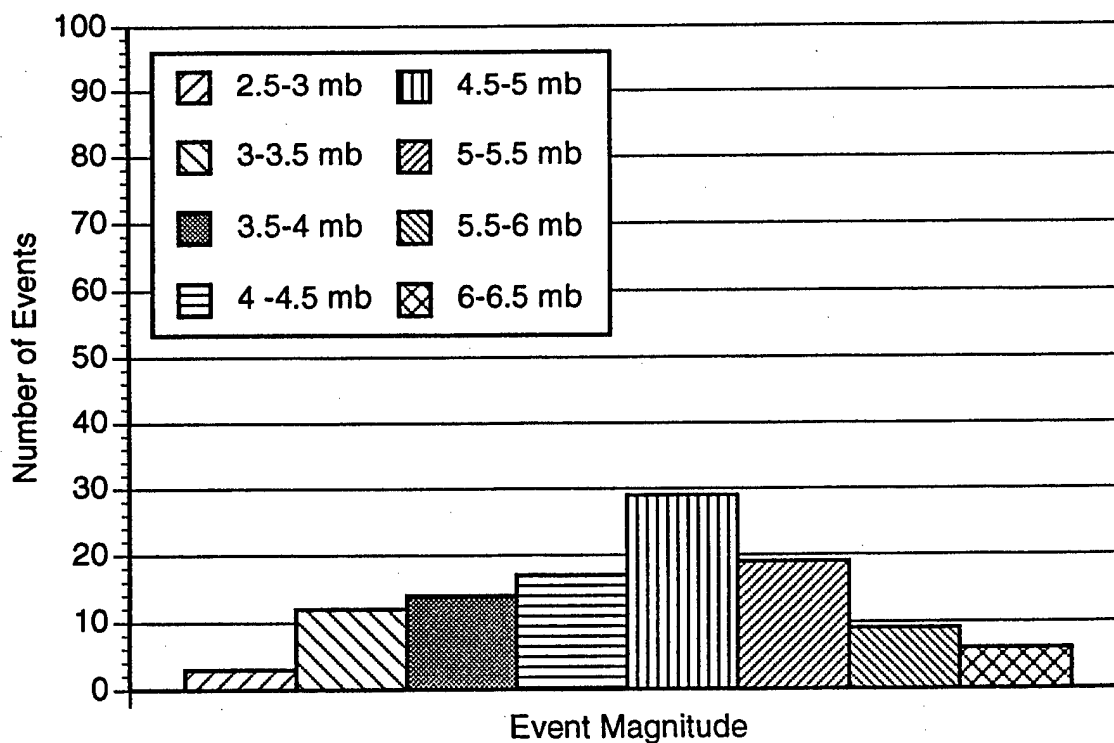


Figure 6. Distribution with respect to magnitude of observations from regional earthquakes in the western U.S. and Eurasia in the current database.

discriminant (cf. Bennett et al., 1996), assuming that  $L_g$  and regional P scale similarly with magnitude.

### **3. Analyses of Empirical Data**

#### **3.1 Background for $L_g/P$ Ratios as Discriminants**

The status of regional seismic discrimination was reviewed by Blandford (1981) and by Pomeroy et al. (1982). Of the 15 discriminant measures considered by Pomeroy et al., the  $L_g/P$  ratio was one of six regional observations assessed to be most promising for event identification. The original observational basis for the use of  $L_g/P$  amplitude ratios as discriminants between underground nuclear explosions and earthquakes was from studies by Willis (1963) and Willis et al. (1963). Willis found that recordings of NTS nuclear explosions and nearby earthquakes observed at a distance of 450 km showed differences in  $L_g/P_n$ ,  $S_n/P_n$ , and  $S_n/P_g$  amplitude ratios, with the largest differences seen for  $L_g/P_n$ . Willis et al., using observations from a global database of explosions and earthquakes, found that nearly 80 percent of the earthquakes had larger  $L_g/P$  ratios than explosions. However, Pomeroy (1977) and Pomeroy and Nowak (1979) found conflicting evidence between observations of  $L_g/P$  for the eastern U.S. and the western areas of the former Soviet Union. While  $L_g/P$  ratios were much larger for earthquakes in the eastern U.S. than for the single nuclear explosion (viz. SALMON), a sample of explosions and earthquakes from the former Soviet Union produced roughly equal  $L_g$  and P amplitudes for both event types. Blandford (1981) was able to achieve substantial success in separating  $L_g/P$  amplitude ratios for western U.S. earthquakes and underground nuclear explosion tests by adjusting the measurements for distance differences, presumably related to attenuation. He found that  $L_g/P$  amplitude ratios were a factor of 3-5 larger for eastern and western U.S. earthquakes than for U.S. nuclear explosions when the observations were adjusted for amplitude decay to a common range of 1000 km. Murphy and Bennett (1982) looked systematically at the  $L_g$  and regional P amplitudes from a sample of NTS explosions and earthquakes within 100 km of NTS recorded at a range of about 530 km and found that the  $L_g/P$  ratios for nuclear explosions and earthquakes had statistically indistinguishable populations. However, it should be

noted that the waveform data in some of these early studies is not always of highest quality and that time-domain observations frequently suffer from bandwidth limitations of the recording systems in use at the time.

Taylor et al. (1989) assessed the variety of regional discriminant measures identified by Pomeroy et al. (1982) on the basis of observations from a large sample of NTS explosions and western U.S. earthquakes recorded at the Lawrence Livermore National Laboratory (LLNL) seismic network surrounding NTS at ranges of 225 km to 400 km from the explosions. These data represent a significant improvement in quality and quantity over previous studies of regional discrimination. They found significant separation in the  $L_g/P_g$  ratios between source types but also noted considerable data scatter and overlap. Bennett et al. (1989) analyzed high-quality data recorded at a single station at somewhat larger regional distances in the western U.S. from a small sample of NTS explosions and regional earthquakes and found that the broadband  $L_g/P$  ratios were larger for the earthquakes than for the explosions. However, band-pass filter analyses of these data demonstrated conflicting results in different frequency bands, suggesting the need for refinement in these measurement techniques.

With regard to  $L_g/P$  ratios for Eurasian events, Bennett et al. (1989, 1992) investigated the ratios for Shagan River, Lop Nor, and Novaya Zemlya nuclear explosions and earthquakes in the same general region with similar epicentral distances recorded at high-quality, mainly far-regional digital stations. They found that the  $L_g/P$  ratios were frequency dependent with the ratios at frequencies of 1 Hz and lower showing similar levels for nuclear explosions and earthquakes, while above 1 Hz the ratios tended to be significantly larger for earthquakes than for explosions. Bennett et al. also found some station-dependent differences in the ratios which could be indicative of propagation effects, but comparisons of the ratios for nearly collocated explosions and earthquakes showed that much of the observed differences could be explained by source excitation differences. Baumgardt and Young (1990) and Dysart and Pulli (1990) investigated  $L_g/P$  ratios for small earthquakes and mine blasts in northern Europe and Scandinavia recorded primarily at near-regional high-quality array stations. They also found that earthquakes normally produced larger ratios than the blasts, but the

implications for discrimination of nuclear explosions are not clear because we have only very limited experience comparing the excitation of  $L_g$  and regional P signals from large industrial blasts and nuclear explosions in similar source environments.

### 3.2 $L_g$ /P Ratio Behavior in the Western U.S.

As noted above, the original development of regional phase spectral ratios as discriminants was based primarily on analysis of near-regional (viz. ranges less than about 800 km) signals from NTS nuclear explosions and earthquakes in the western U.S.; and these data still provide the best controlled sample for comparing the behavior of regional phases from these types of sources. Therefore, the initial phases of this project have focused on additional careful analyses of some of these data. In particular, we computed  $L_g$ /P ratios as a function of frequency using the results of band-pass filter analyses applied to the vertical-component records at the LLNL regional network stations from ten NTS underground nuclear explosions and eight nearby earthquakes. Figure 7 shows the locations of the stations and events. Because of the proximity of the explosions and earthquakes and similarity of paths, we would not expect significant differences in the  $L_g$  and regional P signals due to propagation differences; but we will analyze these effects in greater detail as the research continues. In the band-pass filter processing we have used a set of fairly broad, overlapping filter passbands (cf. Bennett et al., 1989, 1996) throughout most of the analyses. Examples of the results from application of these filters to some typical near-regional records were shown in Bennett et al. (1996) and will not be repeated here. The maximum  $L_g$  and P amplitudes were measured from the filter output in each frequency passband, and the corresponding ratios were computed and plotted as a function of filter center frequency. In the later stages of this project, we plan to investigate alternative filtering procedures as well as different measures of  $L_g$  and regional P signal strength. Because the measurements of  $L_g$  and P are from the same frequency band, we would not expect any effect from instrument response and simplified magnitude-scaling laws would indicate that  $L_g$  and P have similar frequency dependence, so that there should be little effect on their ratio from magnitude differences between events.

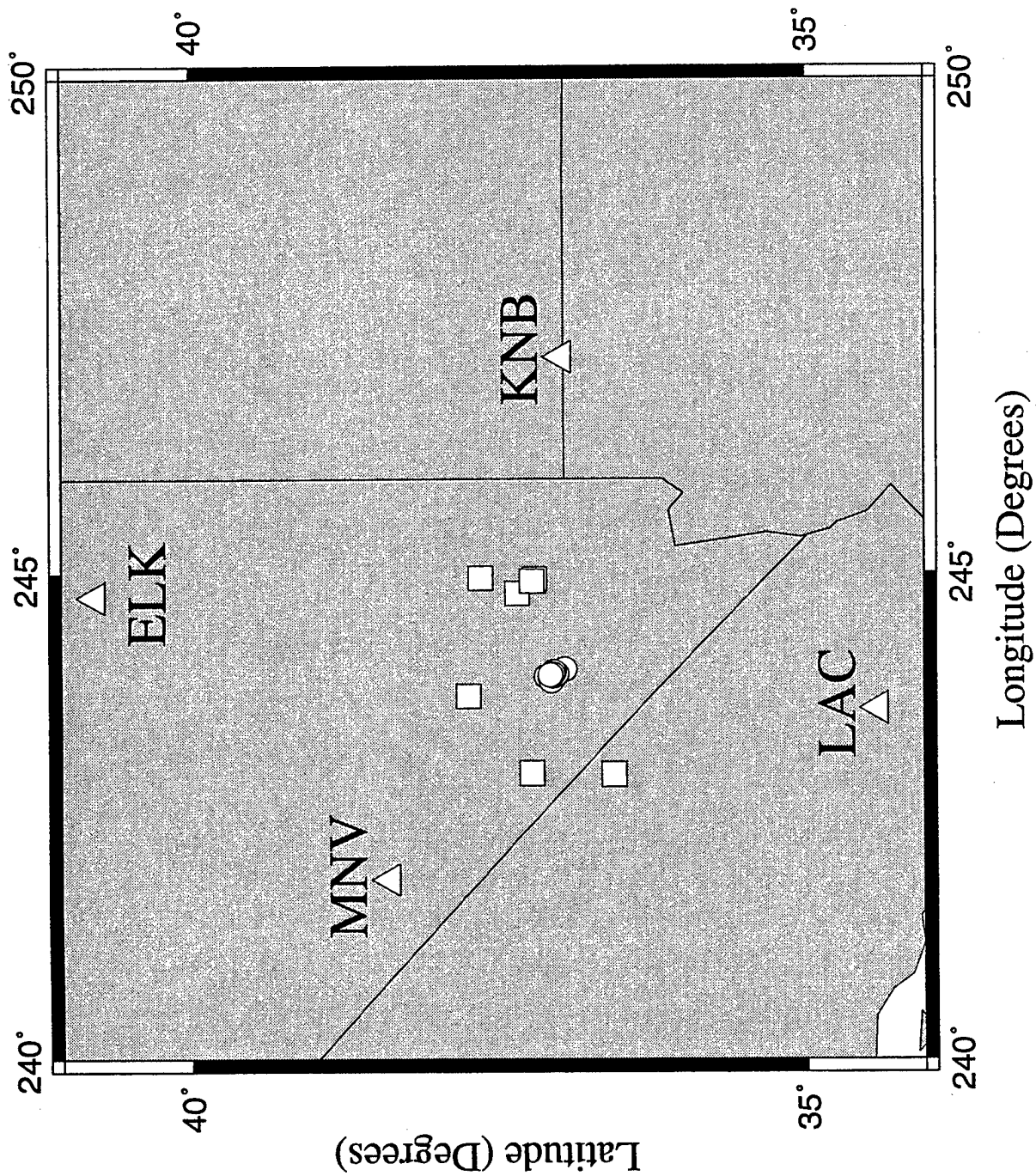


Figure 7. Map showing the locations of NTS nuclear explosions and nearby earthquakes relative to the LLNL network stations.

Figure 8 shows  $L_g/P$  ratios as a function of frequency for eight NTS nuclear explosions recorded at LLNL station KNB ( $R = 290$  km). In general, the ratios have values between one and three at frequencies below about 1 Hz and decline toward higher frequencies. The ratios have values between about one and 0.2 at frequencies above 2 Hz, although there seems to be considerable variability between events. Figure 9 shows similar  $L_g/P$  ratios for five earthquakes recorded at KNB. In this case the ratios have values between two and five at frequencies below about 1 Hz and show only a slight decline with increasing frequency. The earthquake ratios have values between about one and five at frequencies above 2 Hz. Figure 10 shows the  $L_g/P$  spectral ratios averaged over the events for each source type at station KNB. This figure tends to make the general trends more clear; as the average  $L_g/P$  ratio is only about a factor of 1.5 larger for earthquakes at frequencies of 1 Hz and lower, but above about 3 Hz the average  $L_g/P$  ratio is about a factor of five larger for the earthquakes.

In Figure 11, we illustrate the consistency in the average  $L_g/P$  ratios between stations. The plot compares the average  $L_g/P$  ratios as a function of frequency for the NTS nuclear explosion sample recorded at each of the LLNL stations. The average ratios are surprisingly consistent varying by only about a factor of 1.5 around the average determined from all the stations and events. Trends in the slopes of the average curves are notably similar between stations; the biggest differences seem to be in the ratio levels at the individual stations.

Overall the analyses of the western U.S. data indicate that  $L_g/P$  ratios are larger for underground nuclear explosions than for earthquakes. The ratios appear to show more separation between source types at frequencies above about 2 Hz. Over the frequency band analyzed, the earthquake ratios tend to maintain values above one out to high frequencies; while the nuclear explosion ratios drop off more rapidly toward high frequencies to values well below one. One interpretation for this behavior would be that the regional P and  $L_g$  signals have similar spectral content for the earthquake source, but for the explosion source either the high frequency content of  $L_g$  is depleted or the high frequency content of the regional P is enhanced or some combination of these effects prevails. A somewhat troubling aspect of our western U.S. observations from the

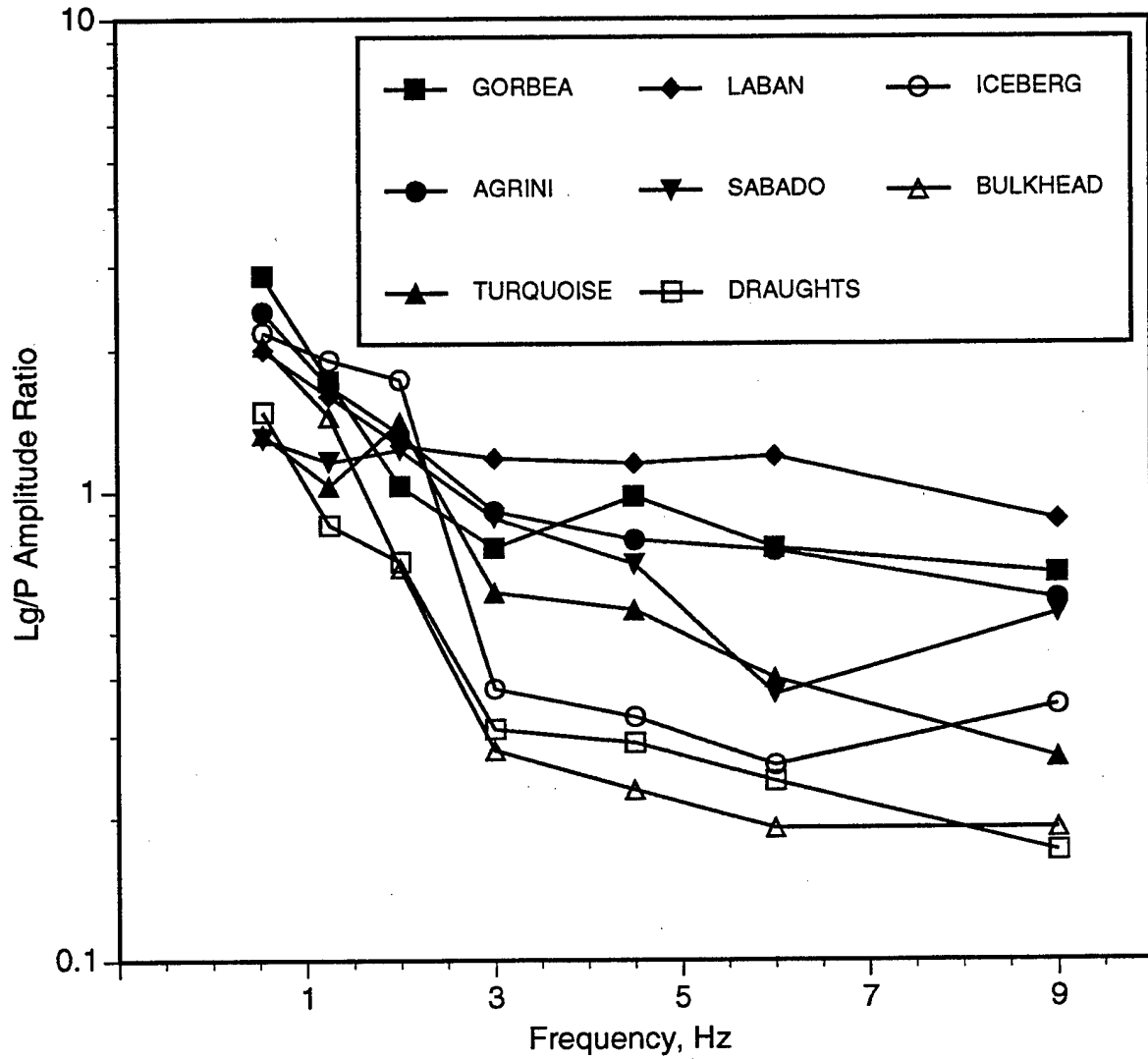


Figure 8. Lg/P amplitude ratios as a function of frequency at station KNB for NTS underground nuclear explosion tests.



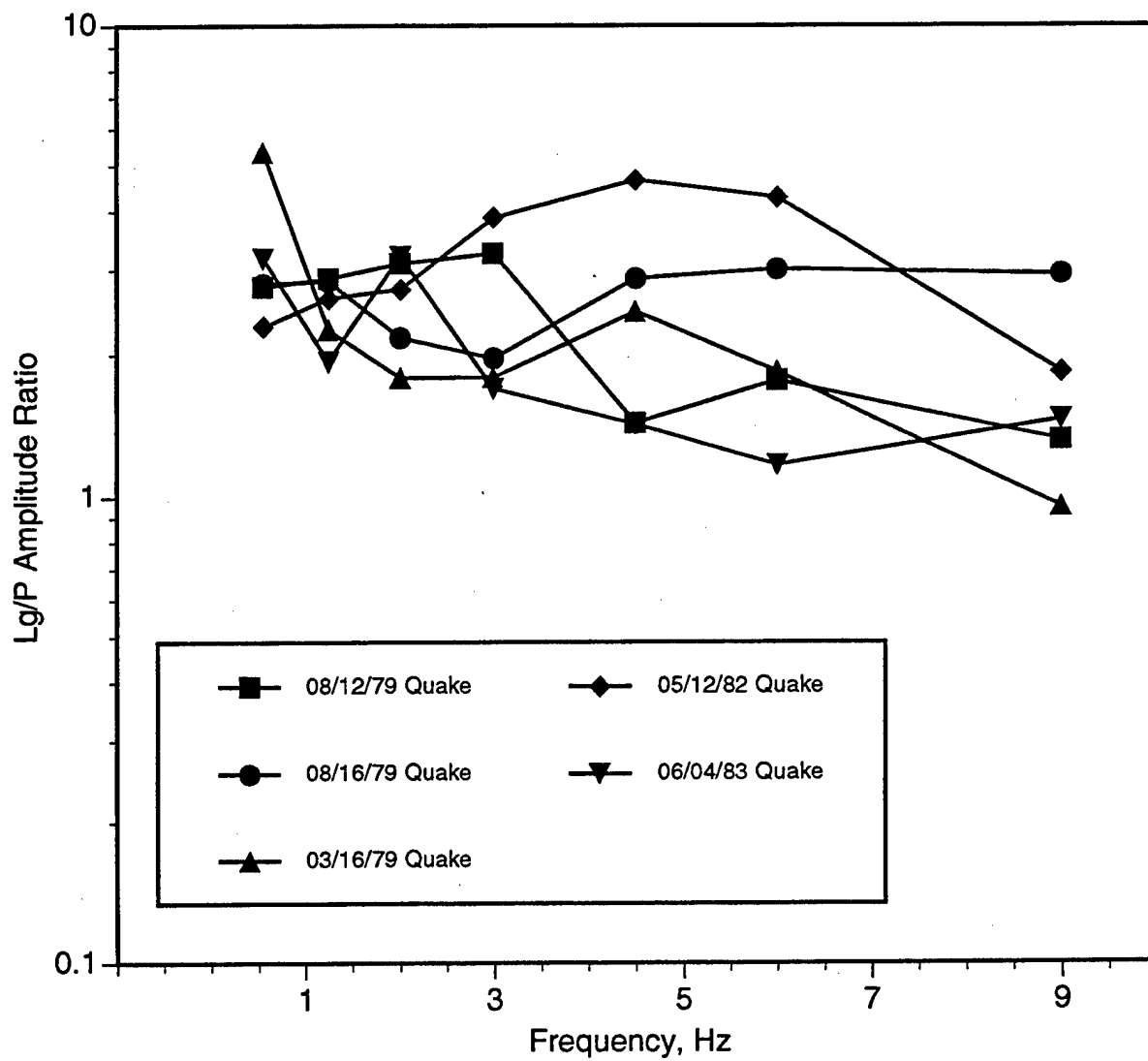


Figure 9. Lg/P amplitude ratios as a function of frequency at station KNB for a sample of earthquakes near NTS.

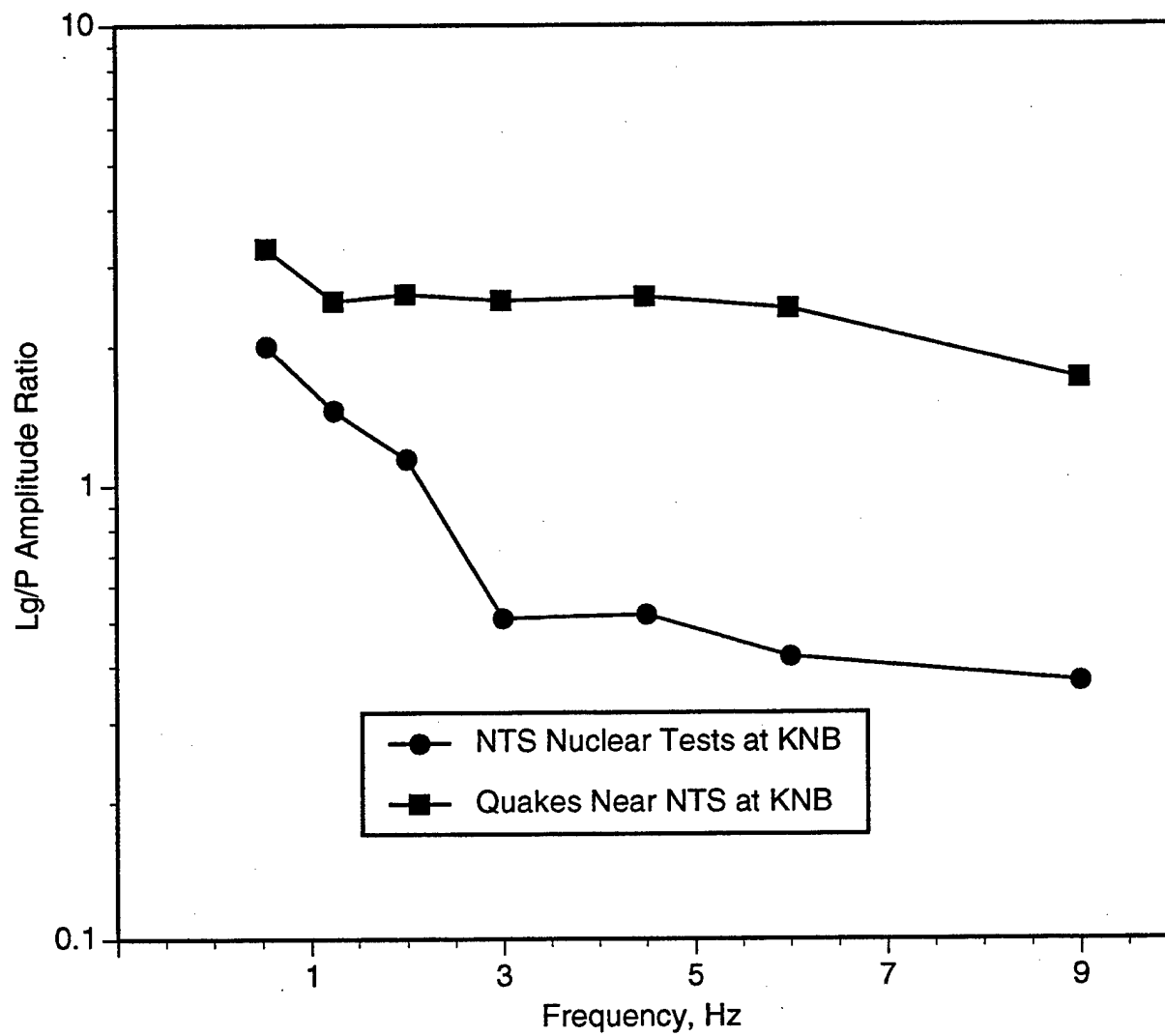


Figure 10. Comparison of average Lg/P amplitude ratios as a function of frequency at station KNB for NTS nuclear tests and nearby earthquakes.

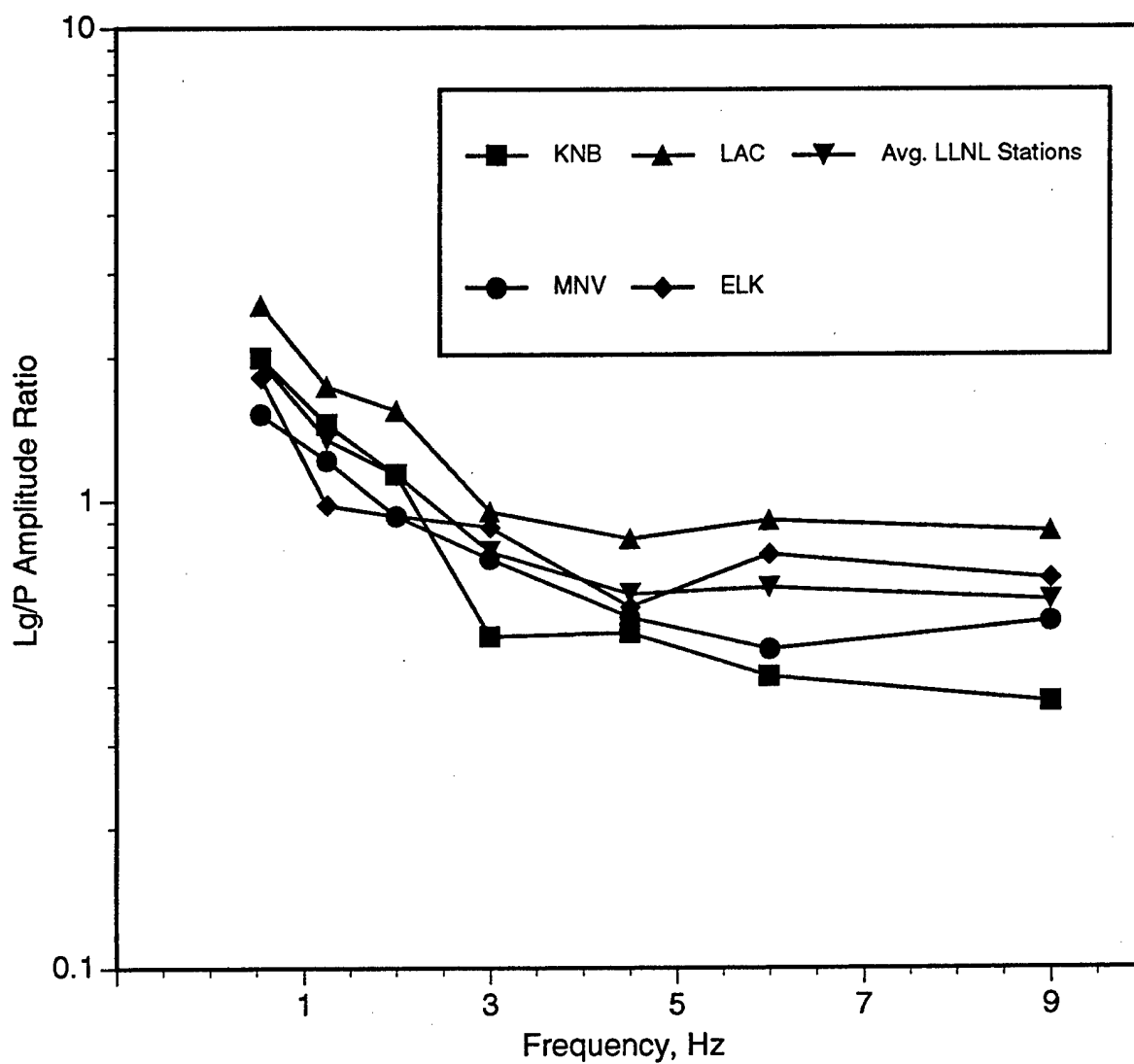


Figure 11. Comparison of average Lg/P amplitude ratios as a function of frequency from each of the LLNL network stations with overall average for ten NTS underground nuclear explosion tests.

standpoint of discriminant reliability is the relatively large scatter in the  $L_g/P$  measurements between sources at a common station. Some of the variations for the earthquakes may be attributable to source or propagation differences between events, but the variability in the explosion ratios would not appear to be related to these factors since the sources and propagation paths are nearly the same from event to event. In fact, the observation of similar average  $L_g/P$  spectral ratios at the different stations when the measurements were averaged over the available explosions seems to suggest that the path differences are relatively small contributors to the overall variability. In the latter phases of this research project, we hope to test some alternative measures of  $L_g$  and P signal strength which may provide more consistent  $L_g/P$  ratios for particular sources.

### 3.3 $L_g/P$ Ratio Behavior in Eurasia

We performed the same band-pass filter analyses to determine  $L_g/P$  spectral ratios for a sample of Eurasian nuclear explosions and earthquakes. We focused our initial efforts for this region on careful analyses of the records at the CDSN station WMQ in China. For many years this station was the nearest regional station to the former Soviet test site at Shagan River, and the sample of data collected at this station from the numerous explosions provide an important link to extend regional monitoring of nuclear explosions to areas outside the western U.S. Figure 12 shows the locations of five Shagan River underground nuclear explosions and five regional earthquakes at similar distances ( $R = 980$  km) relative to WMQ. We used the same, rather broad, overlapping band-pass filters as used in analyzing the western U.S. data and applied them to the vertical-component records at WMQ.

In Figure 13, we show the  $L_g/P$  amplitude ratios as a function of filter center frequency for each of the five explosions and five earthquakes. At frequencies of 1 Hz and below, the  $L_g/P$  ratios have values between about 1.5 and 7; and there is little distinction between the two source types. However, the  $L_g/P$  ratios for the nuclear explosions fall off very rapidly at frequencies above 2 Hz, so that the ratios are between about .05 and .15 for the nuclear explosions. In comparison, above 2 Hz the earthquake  $L_g/P$  ratios fluctuate between about 0.2 and 1.5. So, we again see similar distinctions in

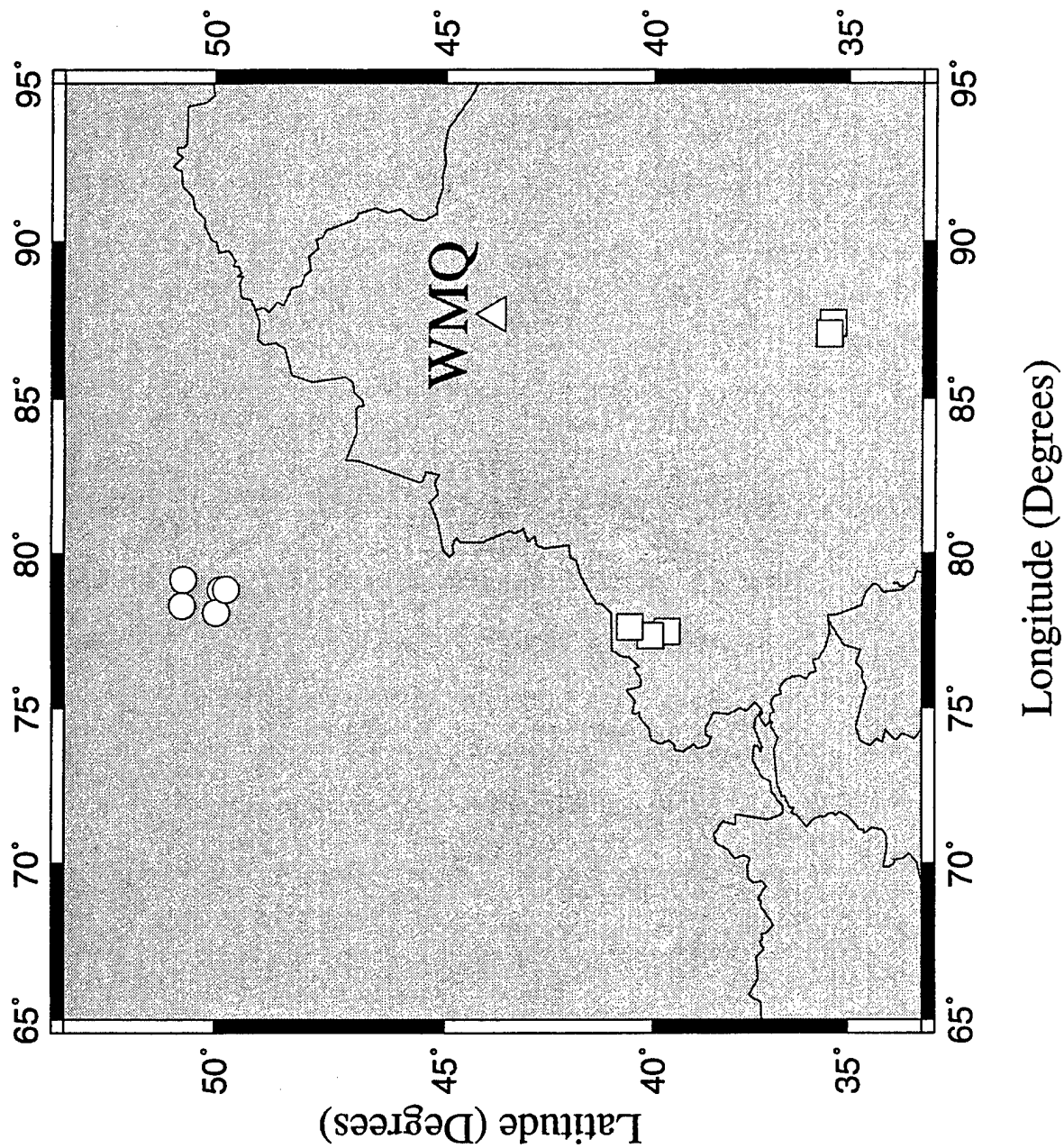


Figure 12. Map showing the locations of Soviet nuclear explosions and nearby earthquakes relative to station WMQ in China.

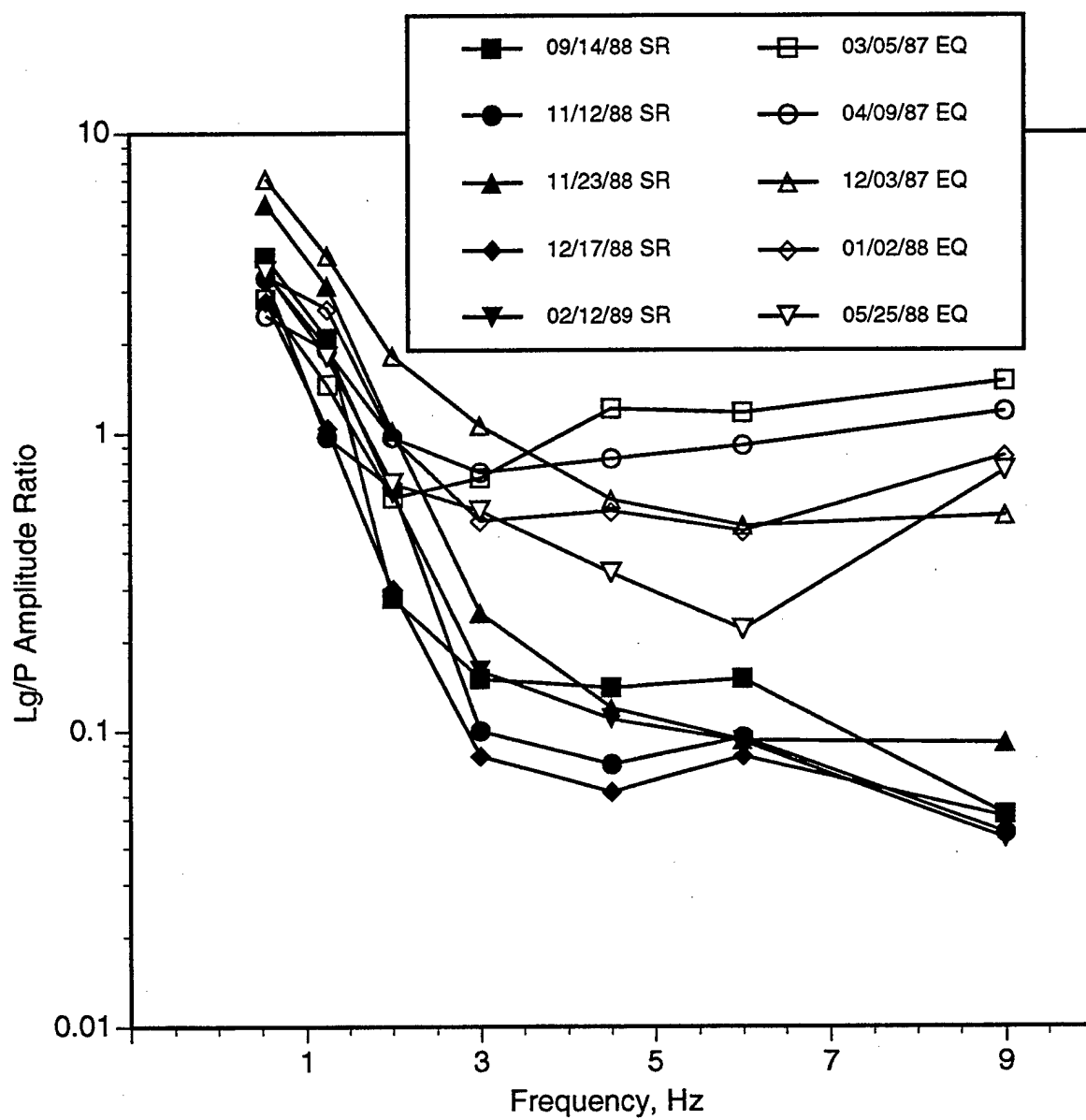


Figure 13. Lg/P amplitude ratios as a function of frequency at station WMQ for Shagan River nuclear explosions and earthquakes at similar epicentral distances.

the  $L_g/P$  ratios with higher ratios for earthquakes than explosions and larger differences at higher frequencies. With regard to consistency between events, the  $L_g/P$  ratios as a function of frequency for the nuclear explosions observed at WMQ are remarkably consistent between events, particularly with regard to the spectral shape. The variability for the explosions here is much smaller than that which we saw above in Figure 8 for the NTS explosions. The variability in the  $L_g/P$  ratios between Shagan River explosions is only about a factor of 2-3 compared to about a factor of 7 for the NTS events in Figure 8. The variability in the earthquake  $L_g/P$  ratios here is about a factor of 5, nearly the same as that seen above in Figure 9 for earthquakes in the western U.S. The largest variations for the earthquakes in both areas are at frequencies between about 4 and 6 Hz.

Figure 14 shows the average  $L_g/P$  ratios determined from the five SR explosions and from the five regional earthquakes. The average ratios are very similar for the explosions and earthquakes at frequencies below about 2 Hz, with values near one. Above 2 Hz the average earthquake  $L_g/P$  ratio remains fairly steady at a value near 0.8-1, while the average explosion  $L_g/P$  ratios fall to values from .07 to .15. So, above 2 Hz the difference between the average explosion and average earthquake  $L_g/P$  ratios at WMQ is a factor of 5 to 14.

To provide some comparisons with other Eurasian nuclear explosions, we computed  $L_g/P$  spectral ratios for five PNEs recorded at regional distances from the high-quality station at Borovoye, BRV; unfortunately no regional records from comparable earthquakes are currently available for this station. The locations of the explosions with respect to BRV are shown in Figure 15. Four of the events are at similar far-regional epicentral distances ( $800 \text{ km} < R < 990 \text{ km}$ ) but at different azimuths around BRV, and the fifth PNE was at a near-regional distance from BRV ( $R = 310 \text{ km}$ ). Figure 16 shows the  $L_g/P$  ratios as a function of filter center frequency for the five PNEs. These ratios generally show more variability than was seen for the Shagan River explosions, and the trends are less clear. There does appear to be an overall decline in the ratios toward higher frequencies. However, the frequency dependence in the  $L_g/P$  ratio is quite different for the nearest PNE (viz. 08/28/73), which suggests that the consistency between events might be improved by adjusting for attenuation differences. Also, some

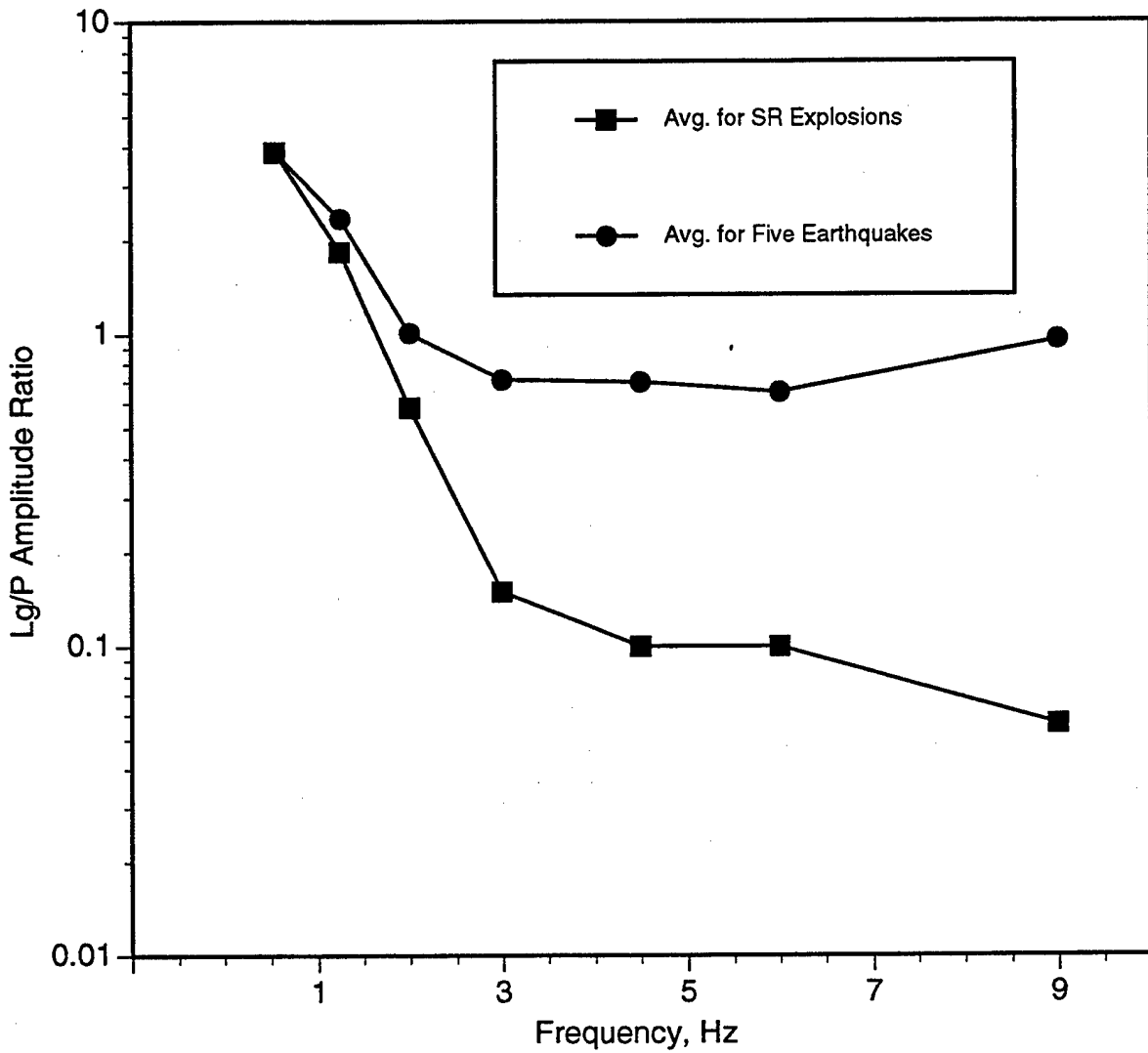


Figure 14. Comparison of average Lg/P amplitude ratios as a function of frequency at station WMQ for five Shagan River nuclear tests and five earthquakes at similar distances.



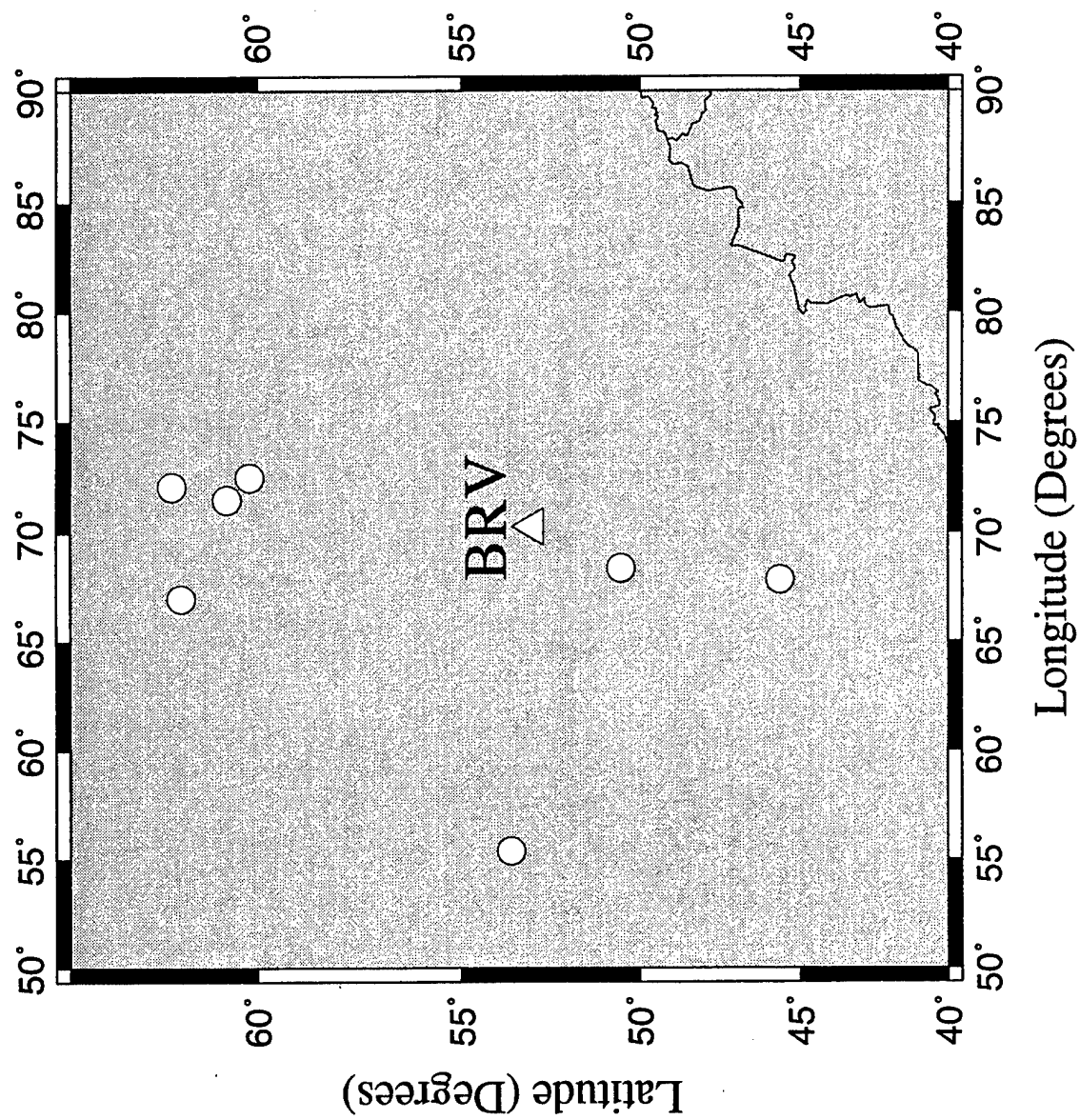


Figure 15. Map showing the locations of selected Soviet PNE explosions relative to station BRV.

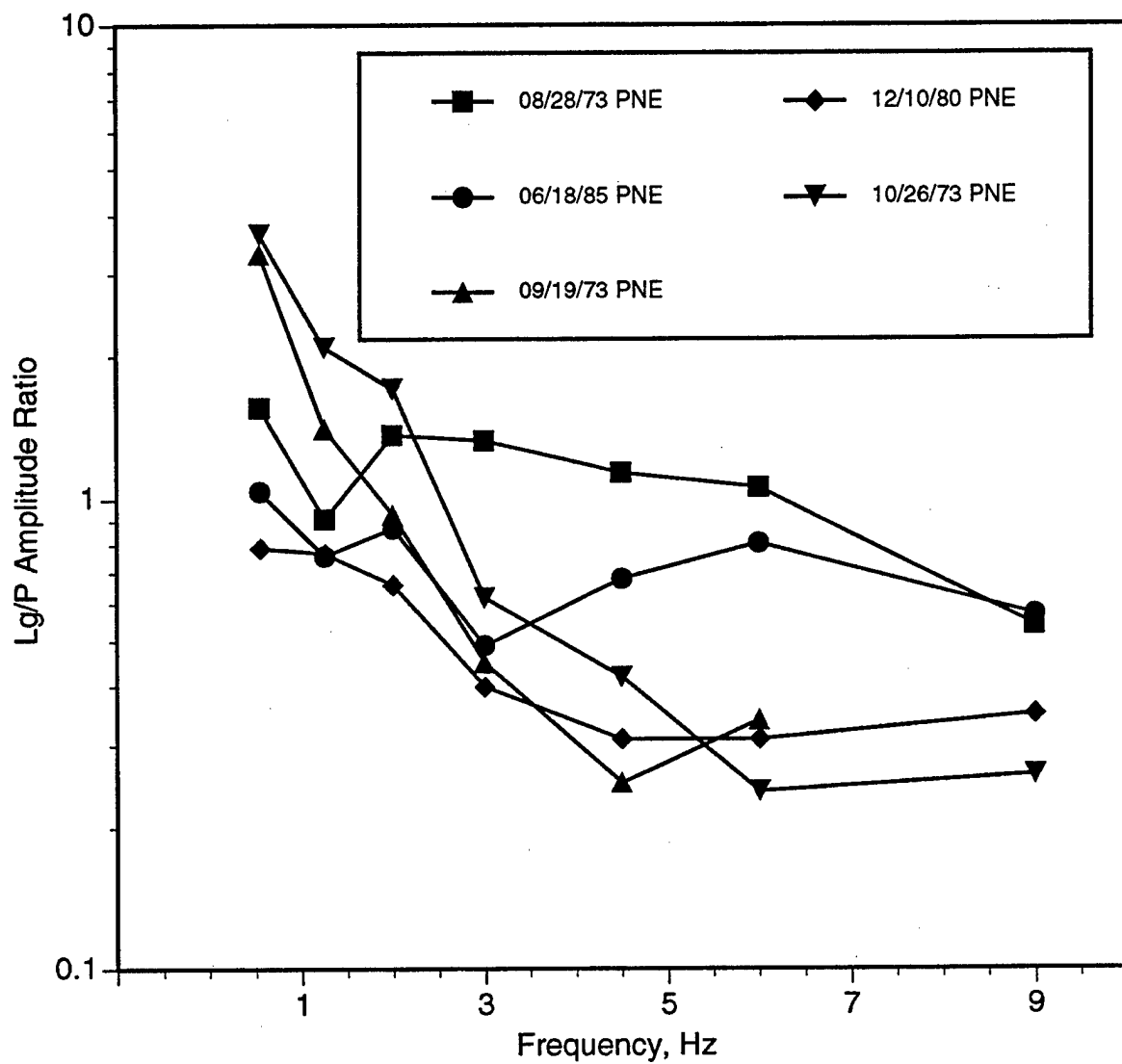


Figure 16. Lg/P amplitude ratios as a function of frequency at station BRV for five PNE tests at epicentral distances less than 1000 km.

unusual azimuthal effects have been noted for the regional signals around station BRV (cf. Murphy et al., 1996; Bennett et al., 1996) which could explain some of the differences in the spectral shapes of the  $L_g/P$  ratios, even though the epicentral distances are similar. In Figure 17, we compare the average  $L_g/P$  spectral ratios for the four PNEs at similar distances recorded at BRV with the average ratios for the five Shagan River underground nuclear tests recorded at WMQ, as shown in Figure 14. The average  $L_g/P$  ratios are fairly similar at frequencies below about 2 Hz and both show fairly rapid decline in levels above 2 Hz; however, the decline is more rapid for the Shagan River events. At frequencies from 3 to 9 Hz, the  $L_g/P$  spectral ratio levels are about a factor of four lower for the Shagan River events than for the PNEs. As noted above, the relatively high  $L_g/P$  ratios for the PNEs could be related to the anomalous azimuthal propagation effects on regional signals around station BRV. In fact, the  $L_g/P$  ratios for the PNEs at southern (viz. 09/19/73) and western (viz. 10/26/73) azimuths from BRV show more rapid fall off in the  $L_g/P$  ratios with increasing frequency and are more similar to the Shagan River event ratios. The PNEs at more northerly azimuths from BRV show a weaker  $P_n$  phase and a strong  $P_g$  phase which are different from the other records (cf. Murphy et al., 1996), and this could be affecting the  $L_g/P$  spectral ratios. We anticipate that some additional refinements in the measurement procedures and adjustments for propagation differences could reduce some of the scatter in the  $L_g/P$  ratios for the PNEs at BRV and increase their similarity to the Shagan River explosions.

### 3.4 Comparisons Between Regions

Finally, as part of the empirical element of this research project, we have sought to make some preliminary comparisons of the behavior of the  $L_g/P$  spectral ratios between different regions. We have made no attempt, as yet, in these comparisons to adjust for differences in observation distance or attenuation which could affect the regional phase spectra and the corresponding spectral ratios. Figure 18 shows average  $L_g/P$  ratios, determined as described above, for several different nuclear explosion samples. In general, the  $L_g/P$  ratios have average values above one at lower frequencies (below about 2 Hz) and then show a decline toward higher frequencies. It is interesting

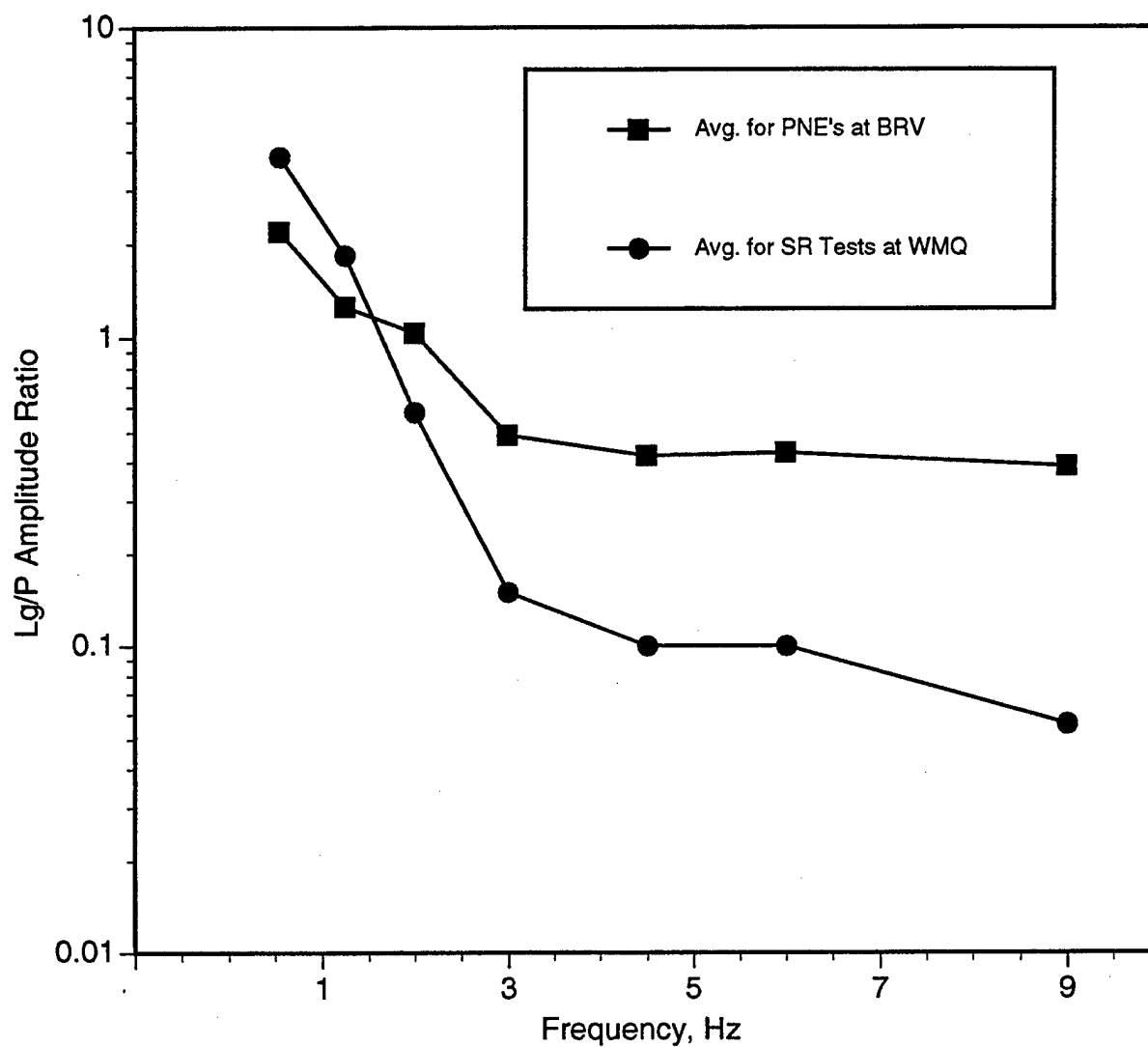


Figure 17. Comparison of average Lg/P amplitude ratios as a function of frequency for four PNE's at station BRV and five Shagan River nuclear tests at station WMQ recorded at similar epicentral distances.

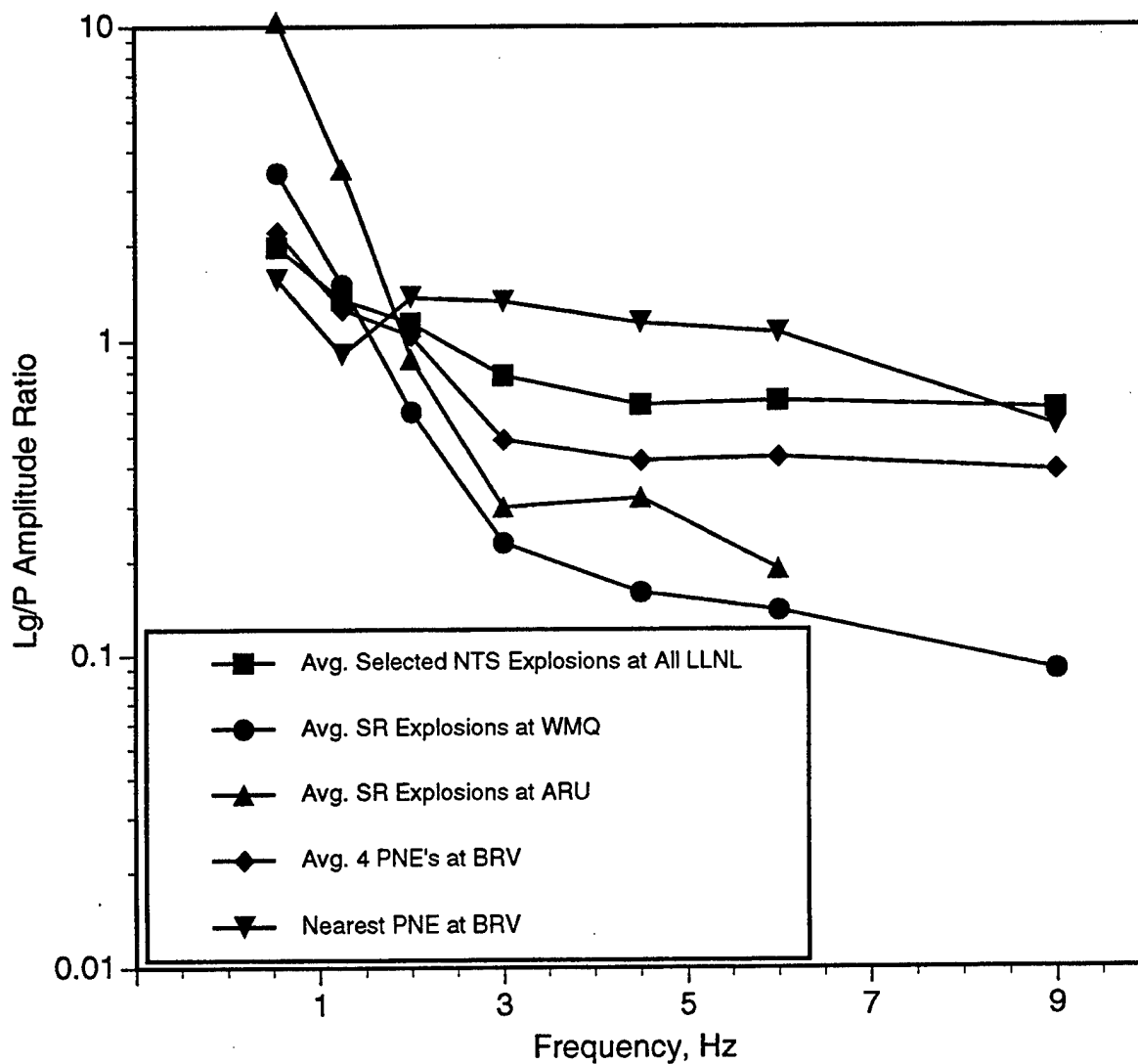


Figure 18. Comparisons of Lg/P amplitude ratios as a function of frequency for selected samples of underground nuclear explosions from several source regions.

to note some of the similarities in the  $L_g/P$  ratio spectral shapes in the figure. First, for the farther regional observations at WMQ ( $R = 980$  km) and ARU ( $R = 1500$  km) from Shagan River underground nuclear explosions, the  $L_g/P$  spectral ratios appear very similar. The values are well above one at low frequencies and then drop off very rapidly with increasing frequencies. There are also strong similarities in the  $L_g/P$  spectral shapes between the average for NTS explosions at all LLNL stations and the average for the four PNEs at similar distances around BRV. There the  $L_g/P$  ratios coincide at low frequencies at values just above one and then decline more slowly with increasing frequencies. The  $L_g/P$  spectral ratio for the single PNE nearest BRV has values near those of the other explosions at low frequencies, but at higher frequencies the ratios tend to be higher for this event. In general, the  $L_g/P$  ratios show sharper decline with frequency for the observations at the farther regional stations. At the nearer stations the ratios still show some decrease with frequency, and the decline seems to be somewhat greater in regions where crustal attenuation is stronger (e.g. vicinity of NTS).

Figure 19 shows average  $L_g/P$  spectral ratios for several earthquake samples. The ratios here are generally larger than those for the nuclear explosions in Figure 18. The ratios tend to be larger where the stations are closer (e.g. near-NTS earthquakes and eastern U.S. events). For the farther regional observations (e.g. earthquakes at WMQ and ARU), the  $L_g/P$  spectral ratios fall off but still tend to remain at or near one at high frequencies. Finally, we show in Figure 20 the  $L_g/P$  spectral ratios for an additional category of events important to CTBT monitoring (viz. rockbursts). Average  $L_g/P$  spectral ratios are shown for rockbursts in three different regions (viz. South Africa, Poland, and eastern U.S.) as measured at selected nearer-regional stations. The spectral shapes in Figure 20 are fairly similar and not much different from those for the earthquakes in the previous figure. The ratios tend to be the greatest at low frequencies (below about 2 Hz) with values in the range 2-5. The  $L_g/P$  values for the rockbursts show a slow decline with increasing frequency with the decrease being slightly greater for the eastern U.S. events.

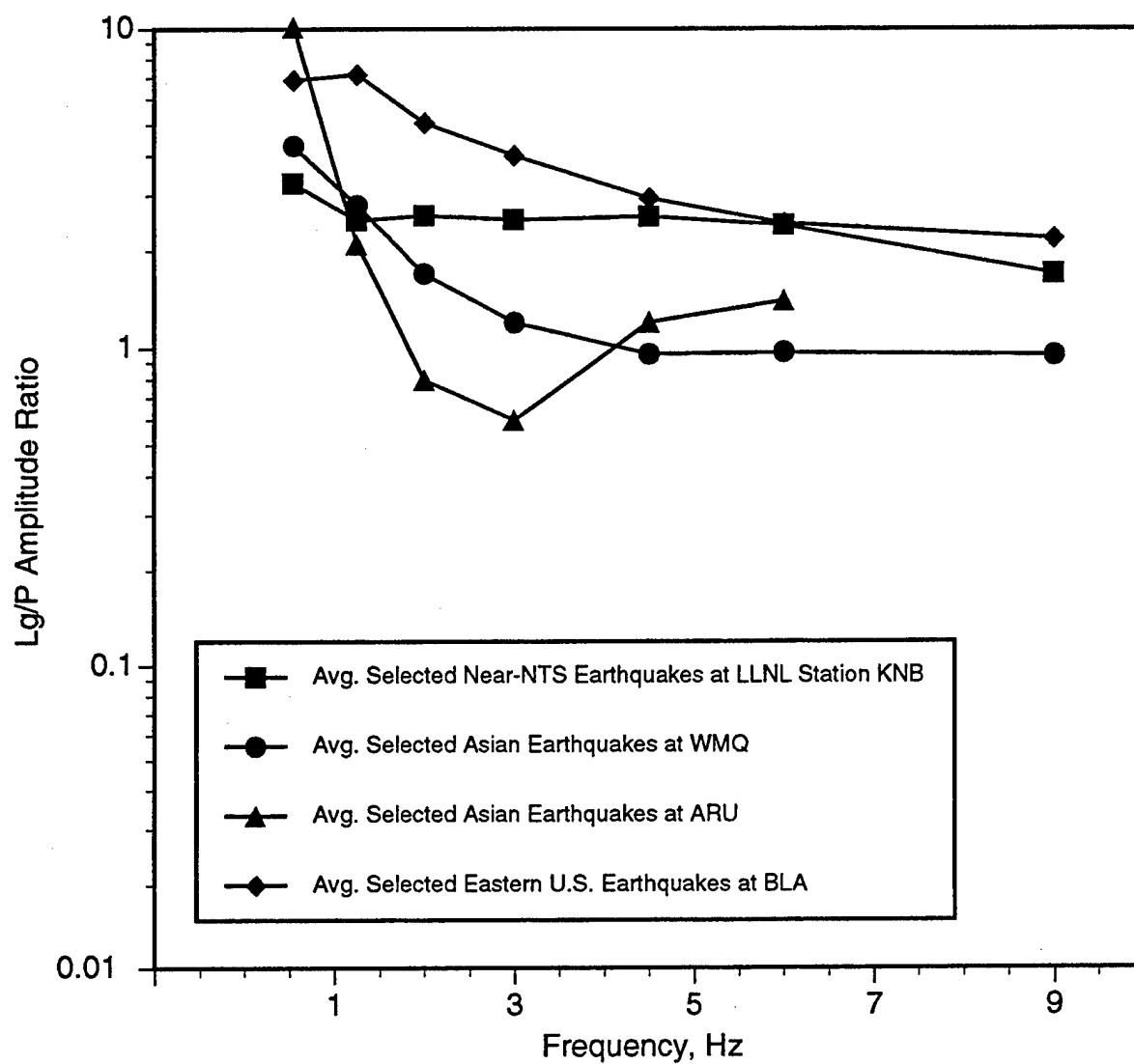


Figure 19. Comparisons of Lg/P amplitude ratios as a function of frequency for selected samples of earthquakes from several source regions.

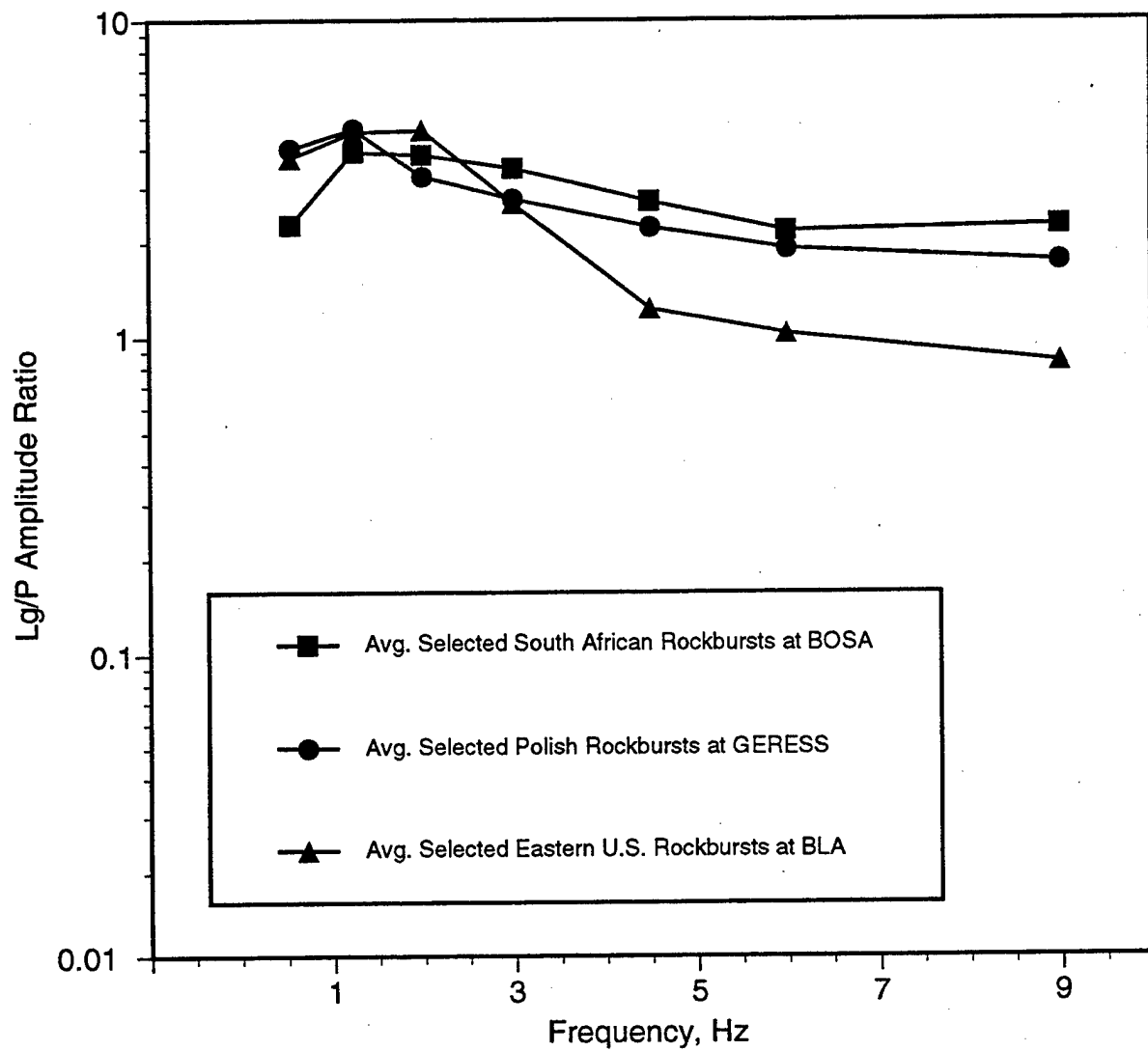


Figure 20. Comparisons of Lg/P amplitude ratios as a function of frequency for rockbursts from several mining regions.



## 4. Theoretical Basis for Understanding of $L_g/P$ Ratios

### 4.1 Modeling Regional Behavior of $L_g$ and P Signals

It is tacitly assumed that explosions show larger  $L_g/P$  ratios because explosions are more isotropic and more efficient radiators of P waves than of S waves. Mechanisms for the generation of regional S and  $L_g$  by explosions fall into two categories. Either they depend upon the conversion of seismic energy radiated by the isotropic source into S waves or they add non-isotropic components into the explosion source. We can list the mechanisms for  $L_g$  generation by explosions as follows:

- $P \rightarrow S$  conversion at the free surface above the isotropic explosion,
- $P \rightarrow S$  conversion at horizontal interfaces near the source,
- $P \rightarrow S$  conversion at non-horizontal interfaces and lateral heterogeneities,
- $R_g \rightarrow S$  conversion by lateral heterogeneities,
- S radiation by the spallation source near the surface above the explosion, and
- non-isotropic S radiation by deviatoric earthquake-like components in the source.

Clearly, all of these mechanisms are at work to some degree or another in any seismic source, and it may be that two or more mechanisms are responsible to a major degree for the differences that we observe in  $L_g/P$  ratios between sources. There are basically three primary observations that we would like to explain with one or more of these mechanisms. First, the consistency of the 0.5-to-1.0 Hz  $L_g$  amplitude versus explosion yield suggests that the mechanism is a stable part of the normal buried explosion source. Second, the  $L_g/P$  ratio near 1 Hz is often larger for earthquakes than for explosions; although our spectral observations from the preceding section suggest that the results at low frequencies are often mixed in some areas. Third, the explosion  $L_g$  spectra fall off faster than earthquakes with increasing frequency. The second observation leads to an  $L_g/P$  ratio discriminant near 1 Hz. The third observation leads to an  $L_g$  spectral slope (or  $L_g$  spectral ratio) discriminant and the improved discrimination capability for  $L_g/P$  ratio measurements at frequencies above 1 Hz.

In this section of the report, we describe theoretical modeling efforts focused on the effectiveness of  $R_g$  to  $L_g$  conversion as a source of the  $L_g$  signals from explosion sources. A recent investigation by Patton et al. (1995) argued that nulls in the  $L_g$  signals near 0.7 Hz from explosions at NTS could be explained by  $R_g$  excited by the spallation source and then subsequently converted from  $R_g$  to  $L_g$ . In this case, the argument presented is that the compensated linear vector dipole (CLVD) source has a null for the excitation of the fundamental Rayleigh wave near 0.7 Hz. The NTS observations indicated that the null was present for normally buried explosion shots that produced spallation, but absent for an over-buried shot that did not produce spallation. We examine in Section 4.2 the feasibility of the hypothesis that  $R_g$ -to- $L_g$  conversion is an important source of  $L_g$  at 1 Hz. It is possible from theoretical considerations to quantify the upper bounds on the amount of  $L_g$  amplitude relative to far-field P-wave amplitude. These bounds are rigid and assume that ALL  $R_g$  energy is converted into P-SV higher modes, which arrive in the  $L_g$  window without scattering into the  $L_g$  coda or into SH higher modes. For two realistic crustal models (viz. NTS and East Kazakhstan), we have found that the upper bounds on the  $L_g/P$  ratio from the  $R_g \rightarrow L_g$  mechanism are comparable to the  $L_g/P$  ratios expected from the explosion source alone generated by  $P \rightarrow S$  conversion at the free surface and by  $P \rightarrow S$  conversion at horizontal interfaces near the source. Since it is likely that the scattered energy will be distributed into SH as well as SV modes, the  $R_g \rightarrow L_g$  scattering mechanism can only at best match these two mechanisms in effectiveness at 1 Hz. Since the  $R_g \rightarrow L_g$  mechanism predicts rapidly decreasing  $L_g$  amplitudes above 1 Hz, it is even less likely that the mechanism contributes significantly to  $L_g$  above 1 Hz.

#### 4.2 Upper Bounds on the Scattering of $R_g$ into $L_g$

It has been suggested by Patton and Taylor (1995) and others (e.g. Jih and McLaughlin, 1988; Gupta et al. 1991; and Xie and Lay 1994) that scattering of short period Rayleigh waves may be a significant source of  $L_g$  from shallow explosions. In a simple layered Earth structure, pure explosion sources only excite  $L_g$  waves by conversion of compressional wave energy at interfaces such as the free surface, and the

conversion of such compressional wave energy to shear-wave energy that will be trapped in the crust as  $L_g$  is inefficient. The P-wave velocity at the explosion's shallow depth of burial (200 to 1000 m) will often be close to or higher than the shear-wave velocity below the Moho ( $\sim 4500$  m/s); and, therefore, the explosion does not excite much P-wave energy at wavenumbers that can be converted to S-waves trapped in the crust by plane layered interfaces. The consistency of  $m_b(L_g)$  as a yield estimator has led researchers to search for a robust mechanism whereby explosion generated seismic energy can be converted into short-period S waves trapped in the crust as  $L_g$ . The strength and reliability of explosion-generated short-period fundamental Rayleigh waves known as  $R_g$  led several researchers to propose the  $R_g$ -to- $L_g$  scattering mechanism as a solution to the explosion-generated  $L_g$  problem. Attenuation for short-period  $R_g$  is strong and probably dominated by scattering from near-surface lateral heterogeneity;  $R_g$  waves at 1 Hz rarely survive to distances of 100 km.

In the following, we estimate the maximum  $L_g$  that could occur from this mechanism assuming that 1) all of the  $R_g$  scatters into P-SV  $L_g$ , and 2) seismic energy is conserved. This analysis leads to an upper bound on the  $L_g$  amplitude that can be produced by the  $R_g$ -to- $L_g$  scattering mechanism.

The vertical displacement from the initial  $R_g$  wave  $u_z^0$  has the form

$$u_z^0(\omega, z, r) = A_0(\omega) \exp(-ikr) E_2(k, z) / \sqrt{r} \quad (1)$$

where  $k$  is the wave number  $\omega/c$ ,  $\omega$  is the angular frequency,  $z$  is the depth,  $E_2$  is the Rayleigh wave vertical displacement eigenfunction which is normalized to 1 at the free surface  $z = 0$ , and  $A_0$  is amplitude spectrum which depends on characteristics of the source and source region earth structure. The radial displacement has a similar form with  $E_2$  replaced by the radial eigenfunction  $E_1$ . The kinetic energy  $T$  in the mode is given by

$$T_0 = \frac{1}{2} \omega^2 \int_0^\infty \rho (|u_z|^2 + |u_r|^2) dz = \frac{\omega^2}{2r} |A_0(\omega)|^2 I_1^0 \quad (2)$$

where  $I_1^0$  is the energy integral on the left with the superscript indicating the fundamental mode.  $I_1$  is the notation used by Takeuchi and Saito (1972) for this integral. In the notation of Harkrider (1964)

$$I_1^0 = \frac{1}{2cUA_R} \quad (3)$$

where  $U$  is the group velocity and  $A_R$  is Harkrider's amplitude factor.

If  $u_z^0$  is now converted to a sum of higher modes, we have

$$u_z^1 = \sum_{i=1}^N A_i(\omega) \exp(-ik_i r) E_2^i(k, z) / \sqrt{r} \quad (4)$$

which using the orthogonality of the modes has a total energy of

$$T_1 = \frac{\omega^2}{2r} \sum_{i=1}^N |A_i(\omega)|^2 I_1^i. \quad (5)$$

So from equations 2 and 5 and the requirement for conservation of energy we have

$$|A_0(\omega)|^2 I_1^0 = \sum_{i=1}^N |A_i(\omega)|^2 I_1^i. \quad (6)$$

Equation 6 constrains the values of  $A_i$ . Although we do not know how much energy scatters into individual modes, we can use this constraint to place some bounds on the  $L_g$  amplitude. If the amplitude of each mode is the same then

$$\left| \frac{A_i}{A_0} \right| = \sqrt{\frac{I_1^0}{\sum_{i=1}^N I_1^i}} = \frac{1}{\sqrt{N}} \sqrt{\frac{I_1^0}{I_1^i}} \quad (7)$$

and if the modes add incoherently, then

$$\left| \frac{u_z^1}{u_z^0} \right|_{\text{even}} \approx \sqrt{\frac{I_1^0}{I_1^i}} \quad (8)$$

The maximum  $L_g$  amplitude will occur if all of the  $R_g$  energy transfers to the single  $L_g$  mode with the minimum energy. In that case we have

$$\left| \frac{u_z^1}{u_z^0} \right|_{\text{max}} \approx \sqrt{\frac{I_1^0}{I_1^{\min}}}. \quad (9)$$

If the energy is equally partitioned among all of the higher modes, then we can expect

$$\left| \frac{u_z^1}{u_z^0} \right|_{\text{equipartition}} \approx \sqrt{\frac{I_1^0}{I_1^i}} \quad (10)$$

Equations 8-10 provide some reasonable upper bounds on the scattering of  $R_g$  into  $L_g$ . It is interesting to note that Eq. 8 and 10 do not explicitly include the number of modes but only averages of the modal energy integrals,  $(I_1^i)$ , and their inverse  $(1/I_1^i)$ .

Figure 21 shows the values of the energy integrals,  $I_1^i$ , calculated at a frequency of 1 hz for the first 10 modes in three earth structures: a Gutenberg Earth model and models for the Nevada Test Site (NTS) and the former Soviet East Kazakh test site (Stevens, 1986). Note that for mode numbers greater than 3 the energy integrals are nearly constant for each model. The energy in these modes is distributed throughout the crust.

The relative amplitudes of Eq. 8-10 are listed in Table 1. For the energy equipartition scattering model, the results are fairly consistent, approximately 15% for each of the three earth models. Scattering ratios vary from about 6% to 50% for the other scattering models. The equipartition model is attractive in that it predicts that the  $L_g$  amplitudes will be approximately the same fraction of  $R_g$  amplitude for all three models.

The numbers in Table 1 represent upper bounds of spectral amplitude of  $L_g$  relative to the predicted spectral amplitude of the fundamental mode not attenuated by scattering. For example, to use these results to compute upper bounds on spectral  $L_g/P$  ratios we must first compute the predicted spectral ratio of  $R_g/P$ . Furthermore, if we wish to use these results to compute upper bounds on the time domain amplitudes we must make some assumptions about the time duration of the  $L_g$  signal. For example we might assume that the  $L_g$  energy is distributed over a group velocity interval from 3.6 to 2.0 km/s and invoke random vibration theory to estimate peak amplitudes. In practice however, the  $R_g \rightarrow L_g$  conversion will probably be more spread out in time and contribute to the  $L_g$  coda as well as the traditional  $L_g$  group velocity window. Another mechanism that may contribute to lower upper bounds of  $L_g$  energy that could be converted from  $R_g$  is the conversion of P-SV  $R_g$  and P-SV  $L_g$  to SH  $L_g$ . It is reasonable to believe that  $R_g$  scattering will contribute to the transverse modes of  $L_g$  as well as the P-SV modes; and,

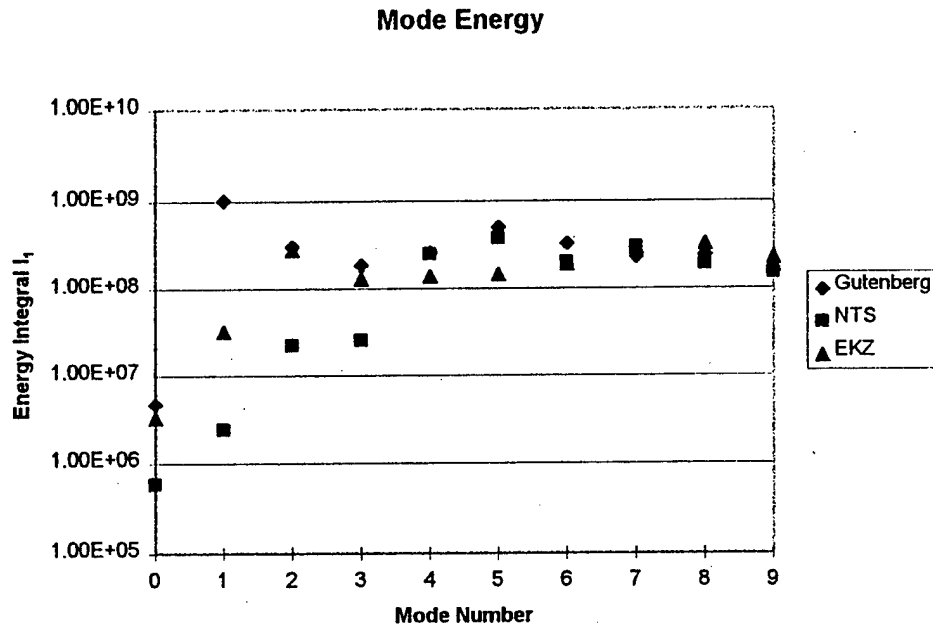


Figure 21. Energy in each mode in three different earth models.

Model	Gutenberg	NTS	EKZ
Equal amplitude	0.114	0.059	0.129
Equipartition	0.131	0.185	0.162
Maximum	0.172	0.494	0.318

Table 1. Scattering ratios for three types of distribution among higher modes: equal amplitude, equipartition of energy, and maximum amplitude in a single mode.

Model	Gutenberg	NTS	EKZ
$L_g/P$ from explosion source	1.7	5.0	3.0
$L_g/P$ $R_g \rightarrow L_g$ scattered from explosion source	11	6.2	8.1

Table 2.  $L_g/P$  amplitude spectral ratios at 500 km for three models from an explosion point source at a depth of 500 m. In each case, the  $R_g \rightarrow L_g$  generated  $L_g$  spectral energy is comparable to the  $L_g$  energy directly excited by the explosion source.

therefore, we can expect perhaps only 50% of the  $R_g$  energy may be available for the P-SV modes of  $L_g$ . Gupta and Blandford (1983) suggested just this equipartition of energy may be taking place between the P-SV and SH modes of  $L_g$  and suggested this as a mechanism for the short-period transverse motion from explosions observed at regional distances.

As an example of the use of these bounds on P-SV  $L_g$  from  $R_g$  scattering, we estimated the spectral amplitude ratios of  $L_g/P$  for the three models at a distance of 500 km at 1 Hz. Figure 22 shows a synthetic vertical component velocity seismogram bandpassed between 0.75 and 1.25 Hz for an explosion point source ( $10^{14}$  Nt-m) at a depth of 500 m. The shear-wave attenuation of the EKZ model has been increased so as to make the intrinsic attenuation of the fundamental mode Rayleigh wave ( $R_g$ ) insignificant. From this seismogram the spectral amplitudes of P,  $L_g$ , and  $R_g$  were measured and tabulated. The spectral amplitude ratio bound can be estimated from  $L_g/P = (R_g/P) * (R_g \rightarrow L_g / R_g)$ , where  $(R_g/P)$  is the ratio of  $R_g$  to P measured from the seismogram in Figure 22 and  $(R_g \rightarrow L_g / R_g)$  is the scattering ratio from Table 1. For the EKZ model we get a ratio of about 8 at 1 Hz. For comparison, the  $L_g/P$  ratio for the point source explosion is 3. If 100% of the explosion  $R_g$  is converted to P-SV  $L_g$ , the  $L_g$  spectral amplitude would nearly double. The results for the three models are summarized in Table 2 assuming the equipartition of modal energy. The  $L_g$  generated by  $R_g$  to  $L_g$  scattering would range from 120% to 640% percent of the direct  $L_g$ . If we consider a CLVD source as suggested by Patton and Taylor (1995) then the  $R_g \rightarrow L_g$  scattered  $L_g$  spectral amplitudes are reduced by 25% for the Gutenberg model and nearly the same for the NTS and EKZ models.

In summary, we have investigated upper bounds on the mechanism of  $R_g$ -to- $L_g$  conversion using simple modal energy integrals assuming only 1) all  $R_g$  energy is converted to P-SV higher modes and 2) all seismic energy is conserved. These upper bounds may be lowered if we consider the additional conversion of  $R_g$  and P-SV modes to SH modes, or P and S energy that leaks out of the crustal wave guide, or intrinsic attenuation of  $R_g$ . Three Earth structures considered all predict approximately the same relative amplitude between the near-field  $R_g$  and the far-field  $L_g$ .

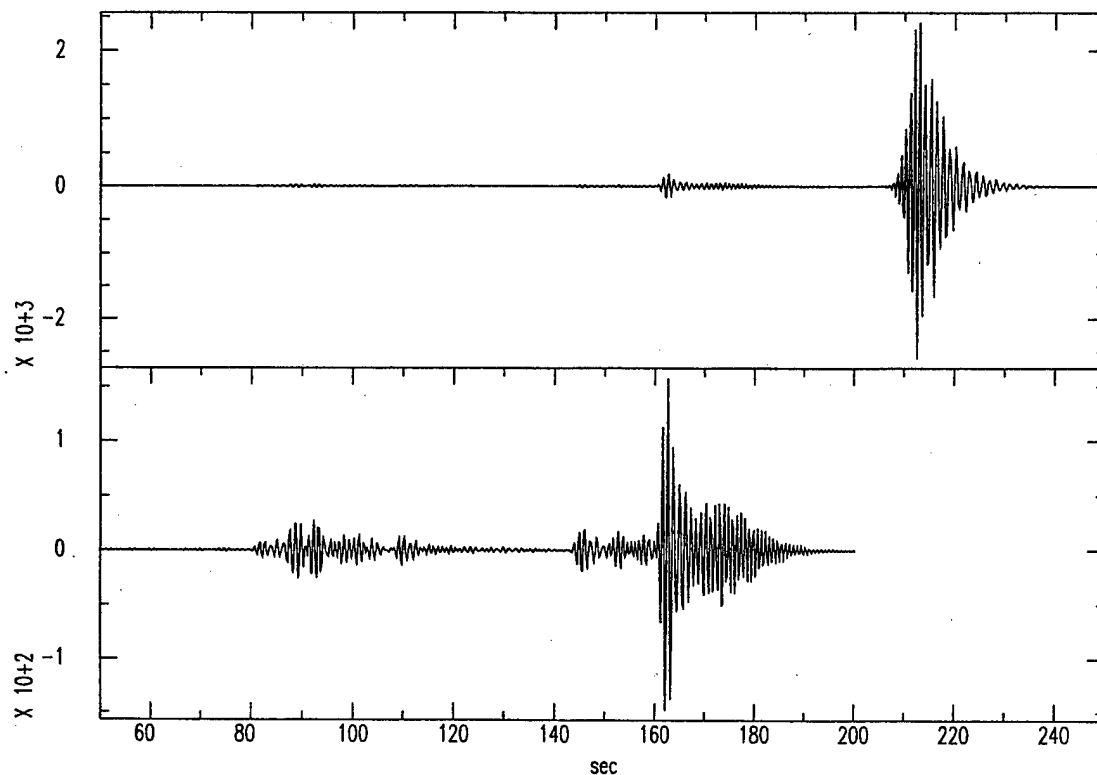


Figure 22. Vertical component synthetic seismogram (0.75-1.25Hz) at a distance of 500km from a  $10^{14}$  Nt-m point explosion source at a depth of 500m in the EKZ model. The upper panel shows the complete synthetic seismogram. The lower panel shows the P and Lg waveforms at a higher magnification. There is 50 times more spectral amplitude in the Rg than the P wave; however, if all of the Rg seismic energy is converted to incoherent higher mode energy, the expected Lg spectral amplitude would only be 270% larger than the direct Lg.



## 5. Summary and Plans

### 5.1 Summary of Main Findings

This research program has involved two principal elements: (1) an empirical element to determine the characteristic behavior of  $L_g/P$  amplitude ratios for the various seismic source types in different tectonic environments, and (2) a theoretical element to analyze the influences of the factors in the different source mechanisms and propagation environments on the  $L_g/P$  ratios and to provide the physical basis for the observed behavior. During the initial phase of this research the empirical element has focused on careful review of the behavior of the  $L_g/P$  ratios and their dependence on frequency for good-quality recordings of regional signals from nuclear explosions in several different tectonic regions, earthquakes at similar regional distances and tectonic environments, and selected alternative source types (viz. rockbursts) in several different regions. The theoretical studies so far have focused primarily on the effectiveness of various mechanisms for generation of  $L_g$  by explosive sources.

In our review of the available regional seismic data, we have collected a large representative database of regional seismic signals from nuclear tests, earthquakes, non-nuclear blasts and rockbursts in a variety of propagation environments. As described in Section 3, we have determined the behavior of  $L_g/P$  amplitude ratios and their dependence on frequency from many of these events and have found that they tend to be consistent with experience indicating larger  $L_g/P$  ratios for earthquakes and rockbursts than for nuclear explosions. Furthermore, the spectral studies show that the differences in the ratios between the source types tend to be greater at higher frequencies (above about 2 Hz). One negative aspect of the observations with regard to discrimination reliability is that, although the average  $L_g/P$  spectral ratios show some clear differences between source types, there seemed to be considerable scatter in the ratios for some of the individual events. In some cases this seemed to be related to possible propagation differences (e.g. for the PNE explosions at different azimuths around station BRV), but we also found some unusual scatter in the ratios for events of similar source type and nearly common propagation paths (e.g. for some of the nuclear tests recorded by the

LLNL network stations). It is hoped that refinements which are being developed for the spectral estimation procedures and regional phase windowing will improve the consistency of the measurements.

In Section 4, we presented theoretical upper bounds on  $L_g/P$  ratios from  $R_g \rightarrow L_g$  scattering for realistic NTS and East Kazakhstan crustal models. We compared these upper bounds at 1 Hz to the expected  $L_g/P$  ratios from an explosion source in a layered-earth model where the  $L_g$  signal is produced by conversion of P waves at the free surface and other horizontal layers. We found that the hard upper bounds from the scattering model are comparable to the explosion  $L_g$  from the alternative model. Since several mechanisms are certainly at work to reduce  $R_g \rightarrow L_g$  scattered energy below the projected upper bounds, we find it likely that the  $R_g \rightarrow L_g$  scattering mechanism is a relatively minor contributing mechanism to  $L_g$  at 1 Hz for nuclear explosions. Furthermore, since the  $R_g \rightarrow L_g$  mechanism theoretically predicts a rapid decline in  $L_g$  amplitude as a function of increasing frequency, it is very unlikely that the mechanism contributes to  $L_g$  at frequencies above 1 Hz. This decrease in  $L_g$  generated from  $R_g$  with increasing frequency results because the  $R_g$  generation by the shallow explosion source declines exponentially at higher frequencies. While this might explain the empirical observation of the rapid decline in  $L_g/P$  ratios from explosion sources with increasing frequency, it is likely that some of the other mechanisms for  $L_g$  or S generation by the explosion could also be controlling the  $L_g$  signal strength in this frequency range. We hope to obtain additional insight into these alternative mechanisms in the continuing stages of this research program.

## 5.2 Plans for Future Work

In the empirical element of this research, we will continue to refine the observational techniques for measuring  $L_g/P$  ratios. We have been looking at alternative spectral measurements of the regional signals and methods for averaging amplitudes over group velocity windows corresponding to the  $L_g$  and regional P for the different propagation regions. We also will be looking more closely at the effects of propagation and attenuation on the regional P and  $L_g$  phases in the different regions and attempting to

define appropriate corrections to the ratio measurements for such propagation effects. These results will then be related to the theoretical behavior expected for the different source types in the different propagation environments. We also intend to look at additional data from more recent events of various source types at several of the seismic stations (e.g. IDC network) which are currently important for monitoring regional events in selected source regions

For the theoretical element of the research program, we will continue over the remainder of the program with our examination of the mechanisms for  $L_g$  production from explosion sources and  $L_g$  propagation in general. We expect to refine the  $R_g \rightarrow L_g$  scattering model and produce frequency-dependent upper bounds on  $L_g/P$  ratios. We have concluded three-dimensional finite difference calculations of regional propagation in crustal models with and without randomized structure. We are in the process of analyzing these calculations and will conduct several more during this year. These calculations examine the propagation of  $P_g$  and  $L_g$  in a three-dimensional crustal waveguide. These calculations will help us address the problem of  $P \rightarrow L_g$  scattering near 1 Hz and the character of  $L_g$  mode-mode conversion. We have been collecting various crustal models for computation of a suite of synthetic layered-earth Green's functions. These models will be used to examine the variability of  $L_g/P$  ratios expected from various sources due to crustal variability. The hypothesis that layering in the crust can be used as a proxy for lateral heterogeneity will be examined using this suite of models.

## 6. References

- Baumgardt, D. R., and G. B. Young (1990). "Regional Seismic Waveform Discriminants and Case-Based Event Identification Using Regional Arrays," *Bull. Seism. Soc. Am.*, 80, pp. 1874 - 1892.
- Bennett, T. J., and J. R. Murphy (1986). "Analysis of Seismic Discrimination Capabilities Using Regional Data from Western United States Events," *Bull. Seism. Soc. Am.*, 76, pp. 1069 -1086.
- Bennett, T. J., B. W. Barker, K. L. McLaughlin, and J. R. Murphy (1989). "Regional Discrimination of Quarry Blasts, Earthquakes and Underground Nuclear Explosions," GL-TR-89-0114, ADA223148.
- Bennett, T. J., A. K. Campanella, J. F. Scheimer, and J. R. Murphy (1992). "Demonstration of Regional Discrimination of Eurasian Seismic Events Using Observations at Soviet IRIS and CDSN Stations," PL-TR-92-2090, ADA253275.
- Bennett, T. J., M. E. Marshall, B. W. Barker, and J. R. Murphy (1996). "Investigations of Regional Phase Spectral Ratios: Transportability and Measurement Algorithms," PL-TR-96-2283.
- Blandford, R. (1981). "Seismic Discrimination Problems at Regional Distances," in *Identification of Seismic Source - Earthquake or Underground Explosion*, D. Reidel Publishing Co., pp. 695-740.
- Dysart, P. S., and J. J. Pulli (1990). "Regional Seismic Event Classification at the NORESS Array: Seismological Measurements and the Use of Trained Neural Networks," *Bull. Seism. Soc. Am.*, 80, pp. 1910 - 1933.
- Gupta, I. N. and R. R. Blandford (1983). "A Mechanism for Generation of Short-Period Transverse Motion from Explosions," *Bull. Seism. Soc. Am.*, 73, pp. 571 - 592.
- Gupta, I. N., T. W. McElfresh, and R. A. Wagner (1991). "Near-Source Scattering of Rayleigh to P in Teleseismic Arrivals from Pahute Mesa NTS Shots," in *Explosion Source Phenomenology*, AGU Monograph 65, pp. 151 - 159.
- Harkrider, D. G. (1964). "Surface Waves in Multilayered Elastic Media, I. Rayleigh and Love Waves from Buried Sources in a Multilayered Elastic Half-Space," *Bull. Seism. Soc. Am.*, 54, pp. 627 - 679.
- Jih, R.-S., and K. L. McLaughlin (1988). "Investigation of Explosion Generated SV Lg Waves in 2-D Heterogeneous Crustal Models by Finite-Difference Method," AFGL-TR-88-0025, ADA213586..

- Murphy, J. R., and T. J. Bennett (1982). "A Discrimination Analysis of Short-Period Regional Seismic Data Recorded at Tonto Forest Observatory," *Bull. Seism. Soc. Am.*, 72, pp. 1351 - 1366.
- Murphy, J. R., D. D. Sultanov, B. W. Barker, I. O. Kitov, and M. E. Marshall (1996). "Regional Seismic Detection Analyses of Selected Soviet Peaceful Nuclear Explosions," SSS-DFR-96-15503, PL-TR-96-2206.
- Patton, H. J. and S. R. Taylor (1995). "Analysis of Lg Spectral Ratios from NTS Explosions: Implications for the Source Mechanisms of Spall and the Generation of Lg Waves," *Bull. Seism. Soc. Am.*, 85, pp. 220 - 236.
- Pomeroy, P. W. (1977). "Aspects of Seismic Wave Propagation in Eastern North America - A Preliminary Report," Rondout Associates Report.
- Pomeroy, P. W., and T. A. Nowak (1979). "An Investigation of Seismic Wave Propagation in Western USSR," Rondout Associates Semi-Annual Technical Report No. 2.
- Pomeroy, P. W., W. J. Best, and T. V. McEvilly (1982). "Test Ban Treaty Verification with Regional Data - A Review," *Bull. Seism. Soc. Am.*, 72, pp. S89 - S129.
- Stevens, J. L. (1986), "Estimation of Scalar Moments from Explosion-Generated Surface Waves," *Bull. Seism. Soc. Am.*, v. 76, pp. 123 - 151.
- Takeuchi, H, and M. Saito (1972). "Seismic Surface Waves," in *Methods in Computational Physics*, Vol. 11, ed. B. A. Bolt, Academic Press, New York, pp. 217 - 295.
- Taylor, S. R., M. D. Denny, E. S. Vergino, and R. E. Glaser (1989). "Regional Discrimination Between NTS Explosions and Western U. S. Earthquakes," *Bull. Seism. Soc. Am.*, 78, pp. 1142 - 1176.
- Willis, D. E. (1963). "Comparison of Seismic Waves Generated by Different Types of Sources," *Bull. Seism. Soc. Am.*, 53, pp. 965 - 978.
- Willis, D. E., J. DeNoyer, and J. T. Wilson (1963). "Differentiation of Earthquakes and Underground Nuclear Explosions on the Basis of Amplitude Characteristics," *Bull. Seism. Soc. Am.*, 53, pp. 979 - 987.
- Xie, X.-B., T. Lay (1994). "The Excitation of Lg Waves by Explosions: A Finite-Difference Investigation," *Bull. Seism. Soc. Am.*, 84, pp. 324 - 342.

THOMAS AHRENS  
SEISMOLOGICAL LABORATORY 252-21  
CALIFORNIA INST. OF TECHNOLOGY  
PASADENA, CA 91125

AIR FORCE RESEARCH LABORATORY  
ATTN: VSOE  
29 RANDOLPH ROAD  
HANSKOM AFB, MA 01731-3010  
(2 COPIES)

AIR FORCE RESEARCH LABORATORY  
ATTN: RESEARCH LIBRARY/TL  
5 WRIGHT STREET  
HANSKOM AFB, MA 01731-3004

AIR FORCE RESEARCH LABORATORY  
ATTN: AFRL/SUL  
3550 ABERDEEN AVE SE  
KIRTLAND AFB, NM 87117-5776  
(2 COPIES)

RALPH ALEWINE  
NTPO  
1901 N. MOORE STREET, SUITE 609  
ARLINGTON, VA 22209

MUAWIA BARAZANGI  
INSTOC  
3126 SNEE HALL  
CORNELL UNIVERSITY  
ITHACA, NY 14853

T.G. BARKER  
MAXWELL TECHNOLOGIES  
8888 BALBOA AVE.  
SAN DIEGO, CA 92123-1506

DOUGLAS BAUMGARDT  
ENSCO INC.  
5400 PORT ROYAL ROAD  
SPRINGFIELD, VA 22151

THERON J. BENNETT  
MAXWELL TECHNOLOGIES  
11800 SUNRISE VALLEY DRIVE, STE 1212  
RESTON, VA 22091

WILLIAM BENSON  
NAS/COS  
ROOM HA372  
2001 WISCONSIN AVE. NW  
WASHINGTON DC 20007

JONATHAN BERGER  
UNIVERSITY OF CA, SAN DIEGO  
SCRIPPS INST. OF OCEANOGRAPHY  
IGPP, 0225  
9500 GILMAN DRIVE  
LA JOLLA, CA 92093-0225

ROBERT BLANDFORD  
AFTAC  
1300 N. 17TH STREET  
SUITE 1450  
ARLINGTON, VA 22209-2308

LESLIE A. CASEY  
DEPT. OF ENERGY/NN-20  
1000 INDEPENDENCE AVE. SW  
WASHINGTON DC 20585-0420

CENTER FOR MONITORING RESEARCH  
ATTN: LIBRARIAN  
1300 N. 17th STREET, SUITE 1450  
ARLINGTON, VA 22209

ANTON DAINTY  
HQ DSWA/PMA  
6801 TELEGRAPH ROAD  
ALEXANDRIA, VA 22310-3398

CATHERINE DE GROOT-HEDLIN  
UNIV. OF CALIFORNIA, SAN DIEGO  
INST. OF GEOP. & PLANETARY PHYSICS  
8604 LA JOLLA SHORES DRIVE  
SAN DIEGO, CA 92093

DTIC  
8725 JOHN J. KINGMAN ROAD  
FT BELVOIR, VA 22060-6218 (2 COPIES)

DIANE DOSER  
DEPT OF GEOLOGICAL SCIENCES  
THE UNIVERSITY OF TEXAS AT EL PASO  
EL PASO, TX 79968

MARK D. FISK  
MISSION RESEARCH CORPORATION  
735 STATE STREET  
P.O. DRAWER 719  
SANTA BARBARA, CA 93102-0719

LORI GRANT  
MULTIMAX, INC.  
311C FOREST AVE. SUITE 3  
PACIFIC GROVE, CA 93950

HENRY GRAY  
SMU STATISTICS DEPARTMENT  
P.O. BOX 750302  
DALLAS, TX 75275-0302

I. N. GUPTA  
MULTIMAX, INC.  
1441 MCCORMICK DRIVE  
LARGO, MD 20774

DAVID HARKRIDER  
BOSTON COLLEGE  
INSTITUTE FOR SPACE RESEARCH  
140 COMMONWEALTH AVENUE  
CHESTNUT HILL, MA 02167

THOMAS HEARN  
NEW MEXICO STATE UNIVERSITY  
DEPARTMENT OF PHYSICS  
LAS CRUCES, NM 88003

MICHAEL HEDLIN  
UNIV. OF CALIFORNIA, SAN DIEGO  
SCRIPPS INST. OF OCEANOGRAPHY  
IGPP, 0225  
9500 GILMAN DRIVE  
LA JOLLA, CA 92093-0225

DONALD HELMBERGER  
CALIFORNIA INST. OF TECHNOLOGY  
DIV. OF GEOL. & PLANETARY SCIENCES  
SEISMOLOGICAL LABORATORY  
PASADENA, CA 91125

EUGENE HERRIN  
SOUTHERN METHODIST UNIVERSITY  
DEPARTMENT OF GEOLOGICAL  
SCIENCES  
DALLAS, TX 75275-0395

ROBERT HERRMANN  
ST. LOUIS UNIVERSITY  
DEPT OF EARTH & ATMOS. SCIENCES  
3507 LACLEDE AVENUE  
ST. LOUIS, MO 63103

VINDELL HSU  
HQ/AFTAC/TTR  
1030 S. HIGHWAY A1A  
PATRICK AFB, FL 32925-3002

RONG-SONG JIH  
HQ DSWA/PMA  
6801 TELEGRAPH ROAD  
ALEXANDRIA, VA 22310-3398

THOMAS JORDAN  
MASS. INST. OF TECHNOLOGY  
BLDG 54-918  
77 MASSACHUSETTS AVENUE  
CAMBRIDGE, MA 02139

LAWRENCE LIVERMORE NAT'L LAB  
ATTN: TECHNICAL STAFF (PLS ROUTE)  
PO BOX 808, MS L-175  
LIVERMORE, CA 94551

LAWRENCE LIVERMORE NAT'L LAB  
ATTN: TECHNICAL STAFF (PLS ROUTE)  
PO BOX 808, MS L-208  
LIVERMORE, CA 94551

LAWRENCE LIVERMORE NAT'L LAB  
ATTN: TECHNICAL STAFF (PLS ROUTE)  
PO BOX 808, MS L-202  
LIVERMORE, CA 94551

LAWRENCE LIVERMORE NAT'L LAB  
ATTN: TECHNICAL STAFF (PLS ROUTE)  
PO BOX 808, MS L-195  
LIVERMORE, CA 94551

LAWRENCE LIVERMORE NAT'L LAB  
ATTN: TECHNICAL STAFF (PLS ROUTE)  
PO BOX 808, MS L-205  
LIVERMORE, CA 94551

LAWRENCE LIVERMORE NAT'L LAB  
ATTN: TECHNICAL STAFF (PLS ROUTE)  
PO BOX 808, MS L-200  
LIVERMORE, CA 94551

LAWRENCE LIVERMORE NAT'L LAB  
ATTN: TECHNICAL STAFF (PLS ROUTE)  
PO BOX 808, MS L-221  
LIVERMORE, CA 94551

THORNE LAY  
UNIV. OF CALIFORNIA, SANTA CRUZ  
EARTH SCIENCES DEPARTMENT  
EARTH & MARINE SCIENCE BUILDING  
SANTA CRUZ, CA 95064

ANATOLI L. LEVSHIN  
DEPARTMENT OF PHYSICS  
UNIVERSITY OF COLORADO  
CAMPUS BOX 390  
BOULDER, CO 80309-0309

JAMES LEWKOWICZ  
WESTON GEOPHYSICAL CORP.  
325 WEST MAIN STREET  
NORTHBORO, MA 01532

LOS ALAMOS NATIONAL LABORATORY  
ATTN: TECHNICAL STAFF (PLS ROUTE)  
PO BOX 1663, MS F659  
LOS ALAMOS, NM 87545

LOS ALAMOS NATIONAL LABORATORY  
ATTN: TECHNICAL STAFF (PLS ROUTE)  
PO BOX 1663, MS F665  
LOS ALAMOS, NM 87545

LOS ALAMOS NATIONAL LABORATORY  
ATTN: TECHNICAL STAFF (PLS ROUTE)  
PO BOX 1663, MS C335  
LOS ALAMOS, NM 87545

GARY MCCARTOR  
SOUTHERN METHODIST UNIVERSITY  
DEPARTMENT OF PHYSICS  
DALLAS, TX 75275-0395

KEITH MCLAUGHLIN  
CENTER FOR MONITORING RESEARCH  
SAIC  
1300 N. 17TH STREET, SUITE 1450  
ARLINGTON, VA 22209

BRIAN MITCHELL  
DEPT OF EARTH & ATMOS. SCIENCES  
ST. LOUIS UNIVERSITY  
3507 LACLEDE AVENUE  
ST. LOUIS, MO 63103

RICHARD MORROW  
USACDA/IVI  
320 21ST STREET, N.W.  
WASHINGTON DC 20451

JOHN MURPHY  
MAXWELL TECHNOLOGIES  
11800 SUNRISE VALLEY DRIVE, STE 1212  
RESTON, VA 22091

JAMES NI  
NEW MEXICO STATE UNIVERSITY  
DEPARTMENT OF PHYSICS  
LAS CRUCES, NM 88003

ROBERT NORTH  
CENTER FOR MONITORING RESEARCH  
1300 N. 17th STREET, SUITE 1450  
ARLINGTON, VA 22209

OFFICE OF THE SECRETARY OF DEFENSE  
DDR&E  
WASHINGTON DC 20330

JOHN ORCUTT  
INST. OF GEOPH. & PLANETARY PHYSICS  
UNIV. OF CALIFORNIA, SAN DIEGO  
LA JOLLA, CA 92093

PACIFIC NORTHWEST NAT'L LAB  
ATTN: TECHNICAL STAFF (PLS ROUTE)  
PO BOX 999, MS K6-48  
RICHLAND, WA 99352

PACIFIC NORTHWEST NAT'L LAB  
ATTN: TECHNICAL STAFF (PLS ROUTE)  
PO BOX 999, MS K6-40  
RICHLAND, WA 99352

PACIFIC NORTHWEST NAT'L LAB  
ATTN: TECHNICAL STAFF (PLS ROUTE)  
PO BOX 999, MS K6-84  
RICHLAND, WA 99352

PACIFIC NORTHWEST NAT'L LAB  
ATTN: TECHNICAL STAFF (PLS ROUTE)  
PO BOX 999, MS K5-12  
RICHLAND, WA 99352

FRANK PILOTTE  
HQ AFTAC/TT  
1030 S. HIGHWAY A1A  
PATRICK AFB, FL 32925-3002

KEITH PRIESTLEY  
DEPARTMENT OF EARTH SCIENCES  
UNIVERSITY OF CAMBRIDGE  
MADINGLEY RISE, MADINGLEY ROAD  
CAMBRIDGE, CB3 0EZ UK

JAY PULLI  
BBN SYSTEMS AND TECHNOLOGIES, INC.  
1300 NORTH 17TH STREET  
ROSSLYN, VA 22209

DELAINE REITER  
AFRL/VSOE (SENCOM)  
29 RANDOLPH ROAD  
HANS COM AFB, MA 01731-3010

PAUL RICHARDS  
COLUMBIA UNIVERSITY  
LAMONT-DOHERTY EARTH OBSERV.  
PALISADES, NY 10964

MICHAEL RITZWOLLER  
DEPARTMENT OF PHYSICS  
UNIVERSITY OF COLORADO  
CAMPUS BOX 390  
BOULDER, CO 80309-0309

DAVID RUSSELL  
HQ AFTAC/TTR  
1030 SOUTH HIGHWAY A1A  
PATRICK AFB, FL 32925-3002

CHANDAN SAIKIA  
WOODWARD-CLYDE FED. SERVICES  
566 EL DORADO ST., SUITE 100  
PASADENA, CA 91101-2560

SANDIA NATIONAL LABORATORY  
ATTN: TECHNICAL STAFF (PLS ROUTE)  
DEPT. 5704  
MS 0979, PO BOX 5800  
ALBUQUERQUE, NM 87185-0979

SANDIA NATIONAL LABORATORY  
ATTN: TECHNICAL STAFF (PLS ROUTE)  
DEPT. 9311  
MS 1159, PO BOX 5800  
ALBUQUERQUE, NM 87185-1159

SANDIA NATIONAL LABORATORY  
ATTN: TECHNICAL STAFF (PLS ROUTE)  
DEPT. 5704  
MS 0655, PO BOX 5800  
ALBUQUERQUE, NM 87185-0655

SANDIA NATIONAL LABORATORY  
ATTN: TECHNICAL STAFF (PLS ROUTE)  
DEPT. 5736  
MS 0655, PO BOX 5800  
ALBUQUERQUE, NM 87185-0655

THOMAS SERENO, JR.  
SAIC  
10260 CAMPUS POINT DRIVE  
SAN DIEGO, CA 92121

AVI SHAPIRA  
SEISMOLOGY DIVISION  
IPRG  
P.O.B. 2286  
NOLON 58122 ISRAEL

ROBERT SHUMWAY  
410 MRAK HALL  
DIVISION OF STATISTICS  
UNIVERSITY OF CALIFORNIA  
DAVIS, CA 95616-8671

MATTHEW SIBOL  
ENSCO, INC.  
445 PINEDA CT.  
MELBOURNE, FL 32940

DAVID SIMPSON  
IRIS  
1200 NEW YORK AVE., NW  
SUITE 800  
WASHINGTON DC 20005

JEFFREY STEVENS  
MAXWELL TECHNOLOGIES  
8888 BALBOA AVE.  
SAN DIEGO, CA 92123-1506

BRIAN SULLIVAN  
BOSTON COLLEGE  
INSITUTE FOR SPACE RESEARCH  
140 COMMONWEALTH AVENUE  
CHESTNUT HILL, MA 02167

TACTEC  
BATTELLE MEMORIAL INSTITUTE  
505 KING AVENUE  
COLUMBUS, OH 43201 (FINAL REPORT)

NAFI TOKSOZ  
EARTH RESOURCES LABORATORY, M.I.T.  
42 CARLTON STREET, E34-440  
CAMBRIDGE, MA 02142

LAWRENCE TURNBULL  
ACIS  
DCI/ACIS  
WASHINGTON DC 20505

GREG VAN DER VINK  
IRIS  
1200 NEW YORK AVE., NW  
SUITE 800  
WASHINGTON DC 20005

FRANK VERNON  
UNIV. OF CALIFORNIA, SAN DIEGO  
SCRIPPS INST. OF OCEANOGRAPHY  
IGPP, 0225  
9500 GILMAN DRIVE  
LA JOLLA, CA 92093-0225

TERRY WALLACE  
UNIVERSITY OF ARIZONA  
DEPARTMENT OF GEOSCIENCES  
BUILDING #77  
TUCSON, AZ 85721

JILL WARREN  
LOS ALAMOS NATIONAL LABORATORY  
GROUP NIS-8  
P.O. BOX 1663  
LOS ALAMOS, NM 87545 (5 COPIES)

DANIEL WEILL  
NSF  
EAR-785  
4201 WILSON BLVD., ROOM 785  
ARLINGTON, VA 22230

RU SHAN WU  
UNIV. OF CALIFORNIA SANTA CRUZ  
EARTH SCIENCES DEPT.  
1156 HIGH STREET  
SANTA CRUZ, CA 95064

JIANG XIE  
COLUMBIA UNIVERSITY  
LAMONT DOHERTY EARTH OBSERV.  
ROUTE 9W  
PALISADES, NY 10964

JAMES E. ZOLLWEG  
BOISE STATE UNIVERSITY  
GEOSCIENCES DEPT.  
1910 UNIVERSITY DRIVE  
BOISE, ID 83725